



# FINAL PUBLISHABLE REPORT

Grant Agreement number 14IND08

Project short name EIPow

Project full title Metrology for the electric power industry

Period covered (dates) From 2015-01-05 To 2018-04-30

Coordinator

Name, title, organisation Dr. Anders Bergman, RISE Research Institutes of Sweden

Tel: +46 10 516 5678

Email: [anders.bergman@ri.se](mailto:anders.bergman@ri.se)

Website address <http://GridMeas.eu>

Other partners

Short name, country

Internal Funded Partners:	External Funded Partners:	Unfunded Partners:
1 RISE, Sweden	6 Aalto, Finland	10 NKT HV, Sweden
2 CMI, Czech Republic	7 ABB, Sweden	
3 PTB, Germany	8 TU Delft, the Netherlands	
4 VSL, the Netherlands	9 TUBS, Germany	
5 VTT, Finland		

## TABLE OF CONTENTS

1	Executive summary .....	3
2	Need for the project.....	4
3	Objectives .....	5
4	Results .....	6
4.1	Objective 1, Ultra-high lightning impulse voltages .....	6
4.1.1	<i>Rationale</i> .....	6
4.1.2	<i>Reference measuring systems with an enhanced voltage range</i> .....	6
4.1.3	<i>Linearity extension methods</i> .....	12
4.1.4	<i>Characterisation of UHV measuring systems</i> .....	14
4.2	Objective 2, Very fast transients.....	18
4.2.1	<i>Measurement of fast transients during puncture testing</i> .....	18
4.2.2	<i>Generation and measurement of fast current steps</i> .....	21
4.3	Objective 3, Losses of power transformers, reactors and capacitors .....	26
4.3.1	<i>Loss measurement on power transformers</i> .....	26
4.3.2	<i>Loss measurement on power capacitors and reactors</i> .....	32
4.3.3	<i>Loss measurement on power cables</i> .....	35
4.4	Objective 4, HVDC convertor station loss.....	39
4.4.1	<i>Rationale</i> .....	39
4.4.2	<i>Measurement of HVDC station power</i> .....	39
4.4.3	<i>Non-invasive current transformer: Prototype compact, distributed digitiser</i> .....	43
4.5	Results summary .....	46
4.5.1	<i>Ultra-high impulse voltage testing</i> .....	46
4.5.2	<i>Very fast transients</i> .....	46
4.5.3	<i>Losses of power transformers, reactors and capacitors</i> .....	47
4.5.4	<i>HVDC convertor station loss</i> .....	47
4.5.5	<i>Collaboration</i> .....	47
5	Impact .....	49
5.1	Dissemination activities .....	49
5.1.1	<i>Scientific publications and trade journals</i> .....	49
5.1.2	<i>Effective cooperation between project partners</i> .....	49
5.1.3	<i>Conferences and relevant fora</i> .....	49
5.1.4	<i>Stakeholder engagement</i> .....	49
5.1.5	<i>Engagement with Standards Development Organisations</i> .....	50
5.1.6	<i>Ecodesign Directive and Market Surveillance</i> .....	50
5.2	Impact on industrial and other user communities .....	50
5.3	Early uptake of project results .....	51
5.4	Impact on the metrological and scientific communities .....	52
5.5	Impact on relevant standards .....	52
5.6	Potential impact .....	52
5.6.1	<i>Instrumentation</i> .....	52
5.6.2	<i>Environmental</i> .....	53
5.6.3	<i>Financial</i> .....	53
5.6.4	<i>Social</i> .....	53
5.6.5	<i>Political</i> .....	53
6	List of publications.....	55
7	Website address and contact details .....	55

## 1 Executive summary

Testing of high-voltage (HV) equipment is routinely performed by the manufacturer to prove that it will withstand the rigours of electrical stresses that can occur in service. Increasing demands on capacity and reliability of the very large energy transmission systems has led to an increase in supply voltages, which has resulted in present-day calibrations not being able to fully cover the required needs. Power electronics involved e.g. in high-voltage DC (HVDC) transmission, pose a need for reliable measurement of current transients, where calibration infrastructure is rudimentary. The international focus on the need to reduce green-house effects has also led to demands on traceable measurement of losses on HV equipment such as power capacitors, reactors, cables and power transformers. In the latter case the European Ecodesign Directive (2009/125/EC) is codified in Regulations as specific requirements on permissible losses. However, present-day infrastructure in these cases is also rudimentary and cannot meet the demands.

In response to these needs this project has developed:

- Reference measuring systems for lightning impulse (LI) up to 1000 kV with best uncertainty for the test voltage value of 0.5 % and 1 % for the time parameters.
- A reference measuring system for very fast transients (VFT) of 500 kV and 200 ns and designed such that a standardised setup for the puncture test is encouraged.
- Calibration facilities for current transients in the sub-microsecond regime at currents up to at least 100 A that have been compared and are now available as services for industry.
- New measurement devices for measurement of losses of power capacitors and reactors which have been verified by intercomparisons.
- Calibration systems for power transformer loss measurement (TLM) systems which have been verified by intercomparisons.
- New methods to perform reliable measurement of the AC resistance of extremely low-loss cables. This is because AC resistance of power cables can be 30-40 % higher than DC resistance..
- Converter stations for HVDC exhibit losses, which have previously only been possible to assess from component tests and estimations. Building on previous work a method and suitable equipment have been identified enabling direct measurement of the loss as the difference between input and output power.

LI calibration capabilities developed in the project, which have been proven to apply at least up to 2700 kV, are now available both for on-site calibration at manufacturers' laboratories and as well as in-house calibrations by the NMI's. New/revised entries to the Bureau International des Poids et Mesures" (BIPM) table for best calibration measurement capability (CMC) will or have been submitted. Findings from the project have been announced in the relevant technical committee of the International Electrotechnical Commission (IEC), TC42, through direct participation. The measuring system for VFT has been adopted by partners VTT, RISE and ABB (formerly STRI) and sold to one external test laboratory, Verescence La Granja in Spain, which uses it in testing of insulators.

Calibration facilities for fast current transients have been developed and verified. The new capabilities will be posted on the CMC tables in the next revision. Communication of the findings to standardisation in IEC TC42, is through the convenor of maintenance team MT12, who is a project partner.

Two reference measuring systems for the calibration of transformer loss measuring systems have been developed, with excellent characteristics that are/will be posted on the CMC tables in their next revision. One of the systems has been demonstrated at a major transformer manufacturer's premises (Smit Transformatoren, the Netherlands) in a full-scale calibration. Feedback from this work to IEC TC14 has been given.

Novel systems for measurement of losses of power capacitors and reactors have been developed based on sampling techniques. This way, lightweight but precise measurement systems have been realised.

The research on losses of power cables has extended previous work to also enable measurement for so-called low-loss cables with individually insulated strands. The results will feed into relevant work in the International Council on Large Electric Systems, (CIGRÉ), where NKT HV is active in WG D1.54 regarding power cable ac resistance measurement and has informed the WG about the activities in this project.

Assessment of loss power of a HVDC converter station was studied in a previous EMRP project ENG07 HVDC. A more general method has been studied now where the AC power and DC power are measured directly with such accuracy that the losses can be calculated. Feedback to standardisation is through the Swedish mirror committees

Finally, in support of station loss measurement, a non-invasive current transformer has been developed to permit live on-site calibration of existing current transformers.

## 2 Need for the project

In the production of equipment for HV grids, dielectric testing is performed to verify that the equipment can withstand the operational environment, including HV and high current impulses. Methods and schemes for calibration have been identified primarily in IEC 60060-2, High-voltage and high-current test techniques. However, system voltages have increased to levels higher than those covered by this standard, and there is an urgent need to extend the traceability of the test methods into the ultra-high voltage (UHV) range. In support of this need, the convenor of the responsible IEC TC42 has stated:

*“...there are several issues related to measurement systems for high voltages, and especially impulse voltages that need to be solved by specialists in measurement techniques. With the increasing test voltages, new needs for calibration techniques emerge, e.g. the need for reliable extension of the result of a calibration at, say, 20 % of the actual test voltage. IEC TC42 would welcome a concerted effort from National Measurement Laboratories to provide solutions in the field of high voltage measurements. Such solutions will inevitably feed into IEC written standards.”*

Traceability of measurements in HV testing is an important tool to ensure high quality and reliability of the tested products. For example, lightning impulse voltage measurement systems are typically calibrated at 500 kV, together with additional measures to extrapolate the linearity up to 2500 kV. Increasing transmission voltage levels requires testing at voltages exceeding 2500 kV, as being studied by CIGRÉ. These increased voltages have led to new demands for calibration, which could not be met with previous methods.

Another extreme in impulse testing is the application of very fast transients, e.g. in puncture testing of insulators for HV lines, where the test voltage can reach 500 kV within a couple of hundred nanoseconds. Prior to the start of this project NMI capabilities, as reported in CMC-tables did not extend to front times below 0.84  $\mu$ s and there were no documentary standards regulating how such calibrations should be carried out. In addition, current, compatibility of tests performed in different locations is questionable and strongly indicated a need for further research and development.

Similarly, NMI capabilities were limited to the measurement of current impulses where calibration requires that characteristics are verified in the sub-microsecond regime (e.g., transformer testing). Prior to this project, NMI capabilities did not extend to the generation of sub-microsecond step currents that exceed 10 A. Furthermore, the latest generation of DC converter valves demanded accurate measurement of fast changing voltage and current signals in order to determine losses. Such switching losses entail measurement of fast current and voltage transients to determine the energy consumed during the switching process.

Loss measurements on large transformers and reactors are performed by manufacturers, using complex commercial measuring systems that rely on extremely precise voltage and current transducers connected to advanced power meters. For large power transformers, it is necessary to measure the active power with an uncertainty of better than 3 %, at a power factor that may be 0.01, which leads to an accuracy requirement of 0.03 % of the apparent power. Piece-wise calibration of the components in the commercial loss measuring system is not sufficient for calibration of such systems since it does not cover possible systematic effects of the overall system and prior to this project there are no calibration facilities in Europe that provide a system calibration service for this purpose with sufficient accuracy (i.e. that is better than 0.01 % or 100  $\mu$ rad in phase).

Triggered by the [Ecodesign Directive](#) and the relevant [Commission Regulation \(EU\) No 548/2014](#), IEC has started a Working Group charged to revise “*Rules for the determination of uncertainties in the measurement of losses in power transformers and reactors*”, which has been under development for some time both in IEC and CENELEC. The coordinator of this project is convenor of this Working Group.

The previous EMRP project ENG07 HVDC, studied the possibilities of measuring losses of converter stations for HVDC and identified a method to do this. Unfortunately, this method required two converters in the same station that can be connected together in such a way that power is circulated between them on a temporary link. In this method the external power fed to the system is a measure of the total loss power, and it can be readily measured. However, such a measurement is rarely possible, (even though project partner RISE has been awarded a contract to perform such a measurement in Sweden) and generally the only alternative for direct measurement is to develop measuring systems that are able to measure the input and output power in both DC and AC sides simultaneously. The accuracy required for this is very demanding and an uncertainty

for both DC and AC power of approximately 0.01 % is needed, at transmission system voltage levels. Currently, it is not clear if this is attainable.

### 3 Objectives

The overall goal for the research has been to underpin sustainability of electrical energy systems in accordance with the aims of the EU's 2020 goals. The goals were sought by improving HV testing of equipment for HV grids, both as regards electrical withstand, and as regards control of electrical losses.

The project therefore had the following objectives;

1. To develop methods to extend the voltage range of traceable LI testing to the ultra-high level of 3500 kV with a target uncertainty of better than 1 %.
2. To develop hardware and methods for the traceable calibration of impulse voltages, using combinations of amplitude and front time, such as those used in puncture testing on insulators (500 kV, 200 ns). As well as, to develop reference calibration circuits for impulse current measuring systems with ultra-fast rise-times in the sub-microsecond range and a peak value range of 50 A to several kA, with 0.5 % uncertainty.
3. To produce facilities for the loss measurement of large power transformers, reactors and power capacitors and AC cables. This should include the measurement of active loss power at low power factors in industrial conditions with extreme phase accuracy of 10  $\mu$ rad and with target uncertainties better than 50  $\mu$ W/VA at voltages and currents up to 150 kV and 2000 A, respectively. Determination of skin effects for three-phase cables will also be studied with the aim to quantify losses incurred.
4. To develop a measurement system for the accurate determination of total HVDC converter station losses by simultaneous measurement of AC and DC power. The target is to measure a 1 % loss with a relative uncertainty of 3 %. In order to facilitate on-site measurements, a non-invasive current sensor should be developed as part of the measurement system with an uncertainty smaller than 50  $\mu$ A/A in current and 50  $\mu$ rad in phase angle.
5. The output of the project will be disseminated via publications in international journals, presentations at scientific and industry conferences, organisation of workshops, and by active participation in international standardisation committees. Together with an active stakeholder committee, this will ensure that the project outputs are effectively disseminated to, and exploited by the electrical power industry and it will facilitate an early take-up of the technology and measurement infrastructure developed by the project.

## 4 Results

### 4.1 Objective 1, Ultra-high lightning impulse voltages

#### 4.1.1 Rationale

Testing of equipment for use in HV grids for electrical transmission is performed to prove that it can withstand over-voltages that can occur in service. Increasing need for energy has driven industry to ever higher transmission voltages, in fact so high that it has been questioned if calibration of measuring systems can be reliably carried out for the highest test voltage now in use in UHV regime, where impulse testing is needed at least up to 2700 kV.

The purpose of this objective was to extend the capabilities of NMI to provide calibration at least up to 20 % of 2800 kV and preferably up to 3500 kV. The goal was to reach 800 kV for reference calibration of LI. In order to prove performance of UHV measuring systems, methods must be available to prove linearity from 20 to 100 % of the maximum voltage, necessitating research into linearity extension methods. Finally, methods to perform the calibration on-site in UHV testing laboratories were identified and validated.

#### 4.1.2 Reference measuring systems with an enhanced voltage range

##### 4.1.2.1 Overview

The existing CMCs before the start of the project were summarised using the “electricity and magnetism” CMCs list of the BIPM.

The branch and service “HV and current” and the sub-service “pulsed HV and current” was chosen. In the individual service “LI” the voltage parameters and the following time parameters were taken into account.

**Table 1: CMCs for Euramet NMIs for LI peak values and time parameters (22.05.2015)**

NMI	LI peak value	Relative expanded uncertainty	Rise time	NMI	front time	Relative expanded uncertainty	time to half	Relative expanded uncertainty	time to chopping	Relative expanded uncertainty
	kV	%	µs		µs	%	µs	%	µs	%
VTT	400	0,5	-	VTT	0.84 - 1.56	1 - 2	40 - 60	0.5 - 1		
LNE	420	0,5	0.8-1.6	LNE	0.8 - 1.6	2.5	40 - 60	1	0.4 - 1.6	5
LNE	420	3	0.4-1.6	PTB	> 0.5	1 - 2	< 60	1 - 2		
PTB	300	0,4	-	INRIM	0.8 - 1.6	3 - 5	40 - 60	3		
PTB	1500	0,5	-	LCOE	0.84 - 1.56	2	40 - 60	1		
PTB	1,6	0,3	-	SP	0.84 - 10	3	40 - 60	3		
INRIM	2	0,7	1,2	UME	0.84 - 1.56	2	40 - 60	2		
INRIM	30	1	1,2							
INRIM	200	1	1,2							
INRIM	700	2	1,2							
LCOE	600	0,5	-							
SP	500	1	1,2							
SP	10	1	>0.2							
UME	1000	1,2	0,84							

##### 4.1.2.2 Capabilities of PTB

The LI impulse measuring systems of PTB consist of LI dividers, connection cables, voltage probes as secondary dividers and transient recorders. A setup for calibration is shown in Figure 1, and a list of dividers available for measurements at PTB is in Table 2.



Figure 1: Setup of the LI calibration of PTB

Table 2 Overview of existing dividers at PTB

Designation	Type	Maximum voltage in kV	Height in m	Manufacturer
PTB1	Damped capacitive	300	1.5	PTB
PTB2	Resistive	2000	8	PTB
PTB3	Damped capacitive	1000	5	PTB
PTB4	Damped capacitive	1500	8	Haefely

A new standard impulse voltage divider (PTB3) was developed in this project by PTB for traceable calibrations up to 1 MV.

The output voltage is restricted by the maximum input voltage of the transient recorder system to be less than 300 V. The response time of the whole divider is required to be suitable for the break-down time of chopped LI, i.e. in the range of few tens of ns.

The electrical circuit of the 1 MV damped-capacitive divider, including the parasitic capacitors  $C_E$  and  $C_S$ , is shown in Figure 2. The whole HV arm consists of two separate modules each with 20 RC-stages. Each stage includes a capacitance  $C_{Hn} = 6000$  pF and a resistance  $R_{Hn} = 7$   $\Omega$ . This results in a capacitance of 300 pF per module and an overall capacitance of 150 pF. With a resistance of 140  $\Omega$  per module and a damping resistance  $RC = 70$   $\Omega$  in the HV connection, the overall HV arm resistance is 350  $\Omega$ , leading to an RC-constant of 52.5 ns. These values are summarised in Table 3.

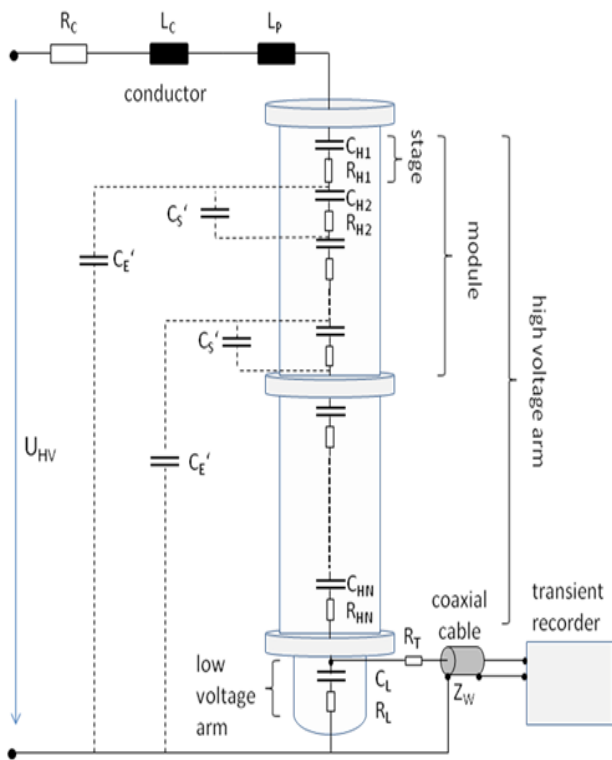


Figure 2 Simplified schematic diagram of the divider including the coaxial cable and transient recorder

To obtain an output voltage value of 300 V the divider needs to have a scale factor of 3333.3. Furthermore, the low voltage arm of the divider must match the HV arm RC-constant of 52.5 ns. This leads to a capacitance  $C_L$  of 500 nF and a resistance  $R_L$  of 0.105  $\Omega$ . Travelling wave reflections are reduced by using a matching resistor  $R_T$  between the low voltage arm and the coaxial cable.

Table 3 Overview of the specific values of the new divider

	conductor& parasitic	per stage	per module	$\Sigma$
Resistance in $\Omega$	70	7	140	350
Capacitance in pF	As shown in Figure 2	6000	300	150
Inductance in $\mu\text{H}$	~12	-	-	~12

There are four measuring instruments at PTB’s HV laboratory: (i) Tektronix DSA 602A, (ii) AMOtronics system with six isolated measuring heads each 100 MS/s and 14 bit, (iii) Dr. Strauss TRAS 200-14 and (iv) a self-made transient recorder system based on the National Instruments PXI-5124 (200 MS/s, 12-bit) digitiser.

4.1.2.3 Capabilities of RISE

The HV laboratory at RISE has two test areas, one area for smaller voltages up to 400 kV and another for voltages up to 2 MV. Three resistive reference dividers for LI are available, (i) one very small for 10 kV, but with very fast response, (ii) one HighVolt SMR 500 kV and (iii) one Passoni Villa for 750 kV. In addition, there are mixed RC dividers from Haefely for nominal voltages of 1 MV and 2.4 MV. The impulse voltage dividers available for measurements at RISE are listed in Table 4.

Table 4 Overview of existing dividers at RISE

Designation	Type	Maximum voltage in kV	Height in m	Manufacturer
	Resistive	10	0.5	RISE
SP1	Resistive	500	3	HighVolt
SP2	Resistive	800	3	Passoni & Villa
SP3	Damped capacitive	2400	12	Haefely

Measurement cables from dividers to transient recorders are 75  $\Omega$  tri-axial camera cables connected with outer and inner screens to earth point of the divider, outer screen to cabinet of transient recorder housing and inner screen to earth point of transient recorder. Secondary proprietary attenuators are mounted directly on the measuring instrument.

The main transient recorder is a National Instrument NI5124 with 12 bit resolution and 200 MSamples/s. It is housed in a screening cabinet with EMC performance up to approximate GHz range. Software for impulse evaluation is proprietary RISE software. A Tektronix 3054 with 500 MHz bandwidth, 9 bit resolution and a maximum sampling rate of 5 GSamples/s is used for measurement of very fast transients.

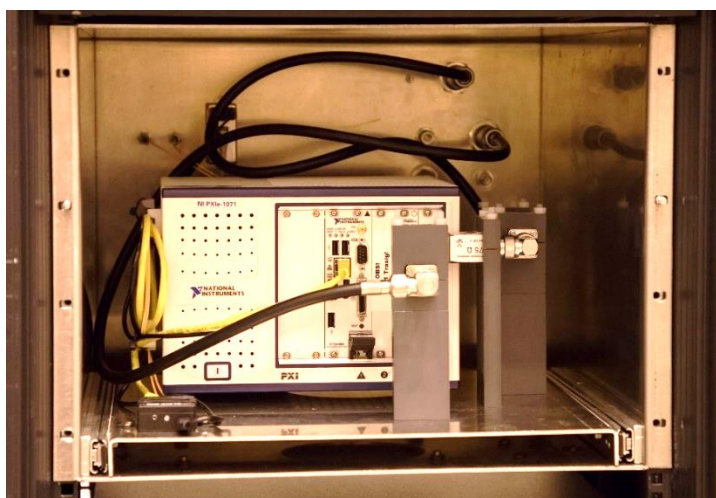


Figure 3: RISE's NI5124 transient recorder in screen box (less front mesh cover)

#### 4.1.2.4 Capabilities of VTT

VTT has capabilities to generate and measure voltages up to 200 kV in their HV laboratory. For higher voltage work, laboratory time is leased from nearby industrial laboratory as needed. LI voltages up to 160 kV are generated using a refurbished Hipotronics IG200-.75 impulse generator.

LI voltages up to 400 kV can be measured using a shielded resistive impulse divider HUT- 400 and National Instruments PXI-5124 (200 MS/s, 12-bit) digitiser. Homemade attenuators are used at the end of the triaxial measuring cable to match the maximum input ranges of the digitisers. The NI digitiser is installed in a rack, which is connected to a PC by a fibre optic cable. The digitiser is controlled with custom software, which corrects the step response of the digitiser by deconvolution and calculates the impulse parameters. The VTT system, which was used as a reference in this project, is shown in Figure 4.

In this VTT system, digitisers are calibrated using a calculable impulse voltage calibrator. Both lightning and switching impulses can be calibrated using different calibrator heads, which generate impulses up to 300 V or 1000 V depending on the type of the calibrator head.



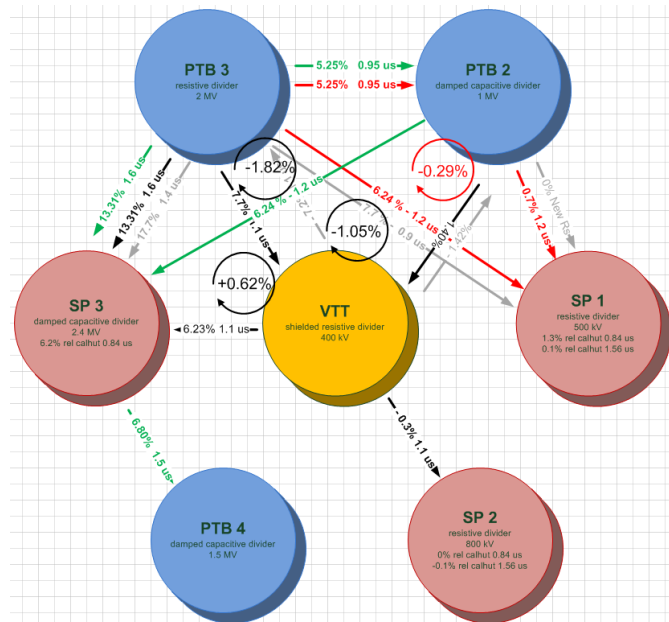


Figure 6 Front time error intercomparison between RISE, VTT and PTB. Values on arrows show the results of one-to-one comparison, and values within circles show the results of closing the triangles.

Resistive dividers often detect the oscillations whereas the damped capacitive (and larger resistive dividers e.g. PTB3) have a slower response and average these out. Often the 30 % point on the front is reached earlier in time than with a curve lacking the oscillations. The resistive dividers detect this shift and the damped capacitive does not. In the Figure 6 below some fronts were faster than others and some contained oscillations. As an example, the error grows from 6.2 to 7.7 % when the front time is shortened from 1.2 to 0.9  $\mu\text{s}$  between PTB3 and SP1.

4.1.2.6 Conclusions

The measurement system comparison in this research project confirms that it is possible to achieve expanded uncertainties of 0.5 % for peak voltage and 1 % for calibration on voltages up to 1 MV. However, it was also observed that even small oscillations on the front of the curve might lead to large front time errors. Large dividers are typically slower, and they do not detect the front oscillations, contrary to fast responding measurement systems. Due to slower response of the large dividers, it was not possible to reach as good agreement on the comparison on voltages from 1 MV to 3 MV. These problems might be to some extent due to the evaluation method defined in IEC 60060-2:2010. Revision of this standard has just been started by IEC TC42, and the project’s findings have been relayed to the committee.

Table 5: Capabilities for the partners after the project

NMI	LI Peak Value	Relative expanded uncertainty	Front time range	Front time	Relative expanded uncertainty	Tail time	Relative expanded uncertainty
	kV	%	$\mu\text{s}$	$\mu\text{s}$	%	$\mu\text{s}$	%
PTB	1000	0.4		>0.5	2	<60	2
RISE	500	0.5	0.84-10	0.84-10	1	40-60	1
RISE	750	0.5	0.84-10	0.84-10	2	40-60	1
VTT	400	0.5	0.84-1.56	0.84-1.56	1-2	40-60	0.5-1

4.1.3 Linearity extension methods

4.1.3.1 *Review of methods*

IEC 60060-2: 2010 describes five methods for extending impulse voltage test value calibration for voltage levels, where reference systems do not exist. One of them does not actually use HV, two others lead to circular definition, and only two are applicable for this study.

One method is based on detecting the field generated by the impulse voltage, and the other on measurement on the DC charging voltage of the generator. These two methods were tested by the project during three measurement sessions described below.

4.1.3.2 *Field probe*

*Damped capacitive divider as a field probe*

Figure 7 shows the ratio between the readings from a PTB damped capacitive divider used as field probe and RISE resistive divider. The PTB damped capacitive divider was not connected to the circuit, but it was placed so that its HV electrode detected the electric field of the impulse. Corona is apparent above 1000 kV where the ratio changes non-linearly. However, there seems to be corona even at lower voltages, as the ratio is not constant. With an accelerating drop of the scale factor above 1000 kV, one can even suspect a presence of streamers. The 1 MV damped capacitive divider worked reasonably well as a capacitive field probe, but only up to a point where corona became apparent.

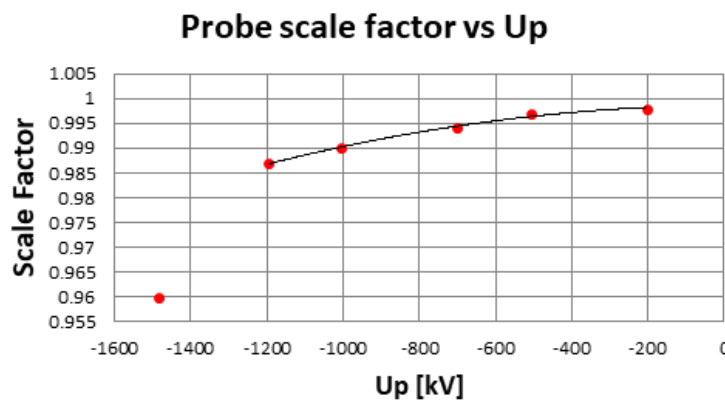


Figure 7: Comparisons between PTB damped capacitive divider as a field probe and RISE 1 MV damped capacitive divider. Vertical scale shows the normalised ratio between the measured test voltage values.

In another test, the RISE 1 MV damped capacitive divider was used as a field probe for studying the linearity of ABB (formerly STRI) 3 MV damped capacitive divider. Figure 8 shows that the results are linear to about +1500 kV using positive polarity, and up to about -2000 kV using negative polarity. Again, we conclude that the field probe suffers from the influence of corona.

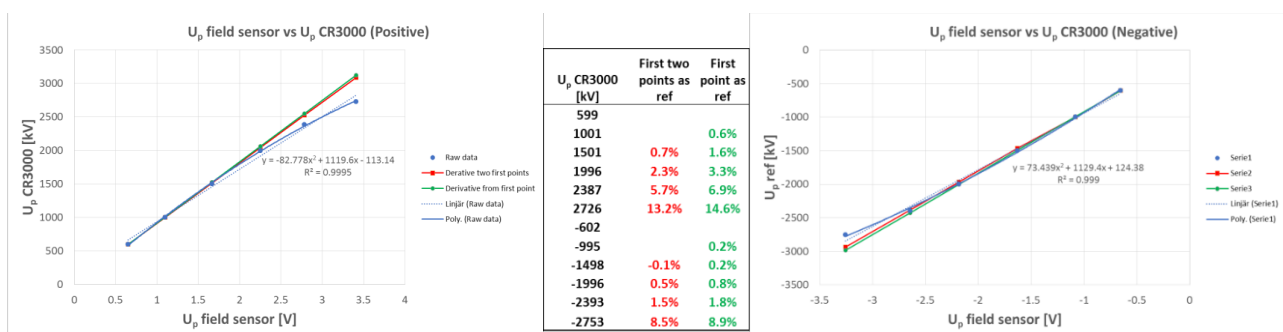


Figure 8: Linearity for positive impulses (left), and negative impulses (right)

### Circuit board as a field probe

Figure 9 shows a comparison between a field probe based on piece of circuit board and the RISE 1 MV damped capacitive divider for -500 kV and -700 kV impulses. An onset of corona, or possibly a small streamer can be seen just before the peak of -700 kV impulse measured by the field probe. One can also see when the discharge extinguishes in the tail at approx. 50  $\mu$ s / -320 kV. As with the divider field probe measurement, the scale factor is also not constant. However, in this case the scale factor is larger than one, meaning we are losing charges detected by the circuit board field probe instead of gaining signal as in the case of the capacitive divider field probe.

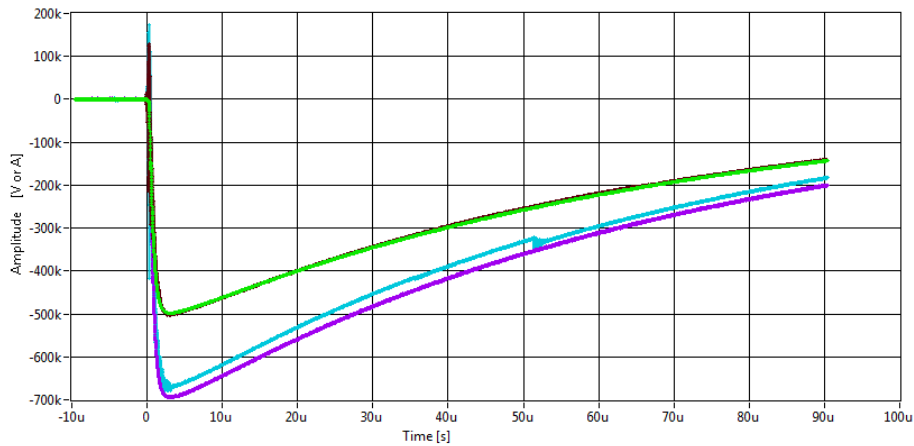


Figure 9: Comparisons between the circuit board as a field probe and the RISE mixed divider. Black and blue: -500 kV and -700 kV impulses measured by the field probe. Green and violet: Respectively for mixed divider.

### Linearity by charging voltage method

In this method the DC charging voltage of a multistage impulse voltage generator is measured before the triggering of each impulse. First the built-in DC measurement of the control unit measuring was calibrated using reference dividers as shown in Figure 10. The charging voltage measurement of the bipolar charging was calibrated using two dividers.

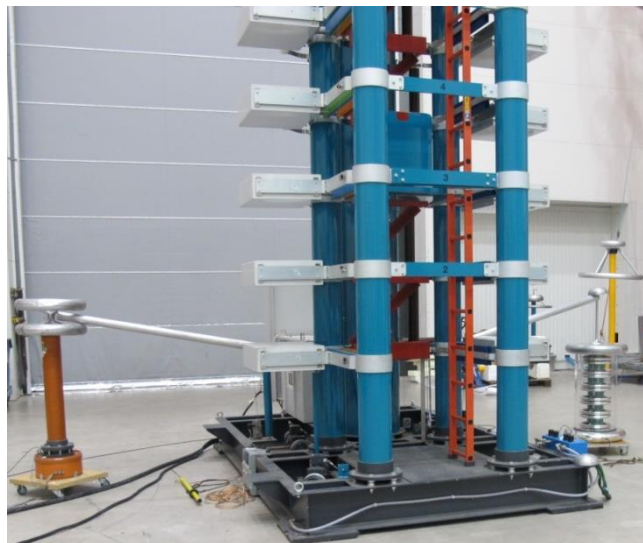


Figure 10: Calibration of the charging voltage measurement of impulse generator. Base of multistage impulse voltage generator in the centre, with the two calibration dividers connected by aluminium tubes on both sides.

Figure 11 shows the result of a comparison between the generator charging voltage and the test voltage value measured by the 3 MV damped capacitive divider. The figure shows the ratio deviation from a reference value.

Three different references were tested, with very similar outcomes. Using method 3 (i.e. linear regression line).we have linearity within 1 % to full voltage and both polarities.

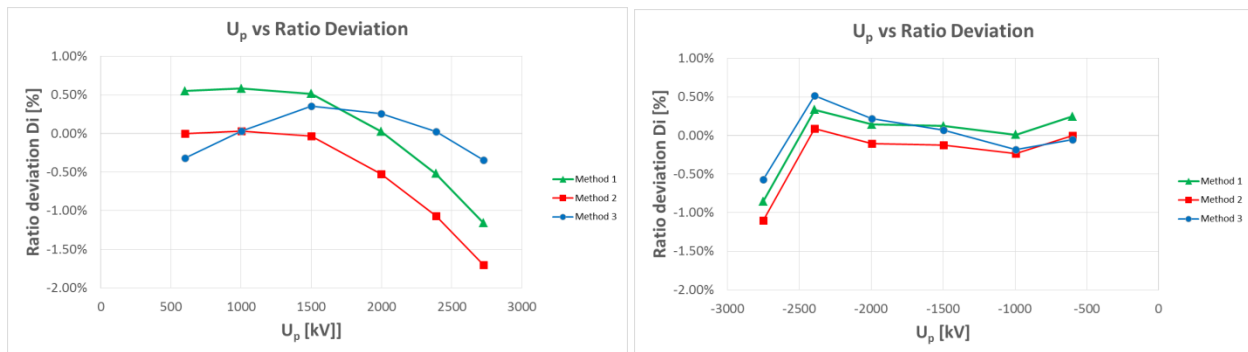


Figure 11: The curves show the deviation from the apparently linear curves when plotting impulse generator charging voltage against the CR3000 measured impulse for both polarities. for positive polarity (left) and negative polarity (right). Ratio deviation is referenced to mean of all readings (method 1), to reading on lowest voltage (method 2), or linear regression line (method 3).

#### 4.1.3.3 Conclusions

One 3 MV divider was found to be linear within  $\pm 1\%$  for voltages up to 2.7 MV. The charging voltage method was found to work best for the determination of linearity of a UHV divider. The charging voltage method works well, when care is taken that all levels of the generator are fully charged. The field sensor method is difficult to use for UHV systems, as corona will cause significant interference. However, this means a field probe is a good tool for corona detection.

#### 4.1.4 Characterisation of UHV measuring systems

##### 4.1.4.1 General

The aim was to provide tools to characterise UHV class dividers, in particular using their pulse response. A characterisation of the pulse response was performed at low voltages, thus allowing investigation of many possible spatial arrangements in a reasonable time-frame. The methods were applied, together with IEC 60060-2:2010 compliant calibrations, to actual (on-site) UHV dividers to determine the achievable accuracy.

The step response of each measuring system was measured on each setup used during HV measurement. These step responses were then used in simulations, in order to predict the errors during actual HV measurements.

##### 4.1.4.2 Study of influencing factors of a 2 MV damped capacitive divider

###### Divider connection

Various geometries for the connection between small lower voltage reference divider and large higher voltage test divider are shown in Figure 12. For step response measurement the step generator was placed on the feed point, where the lead from impulse generator meets the input leads of the two dividers.

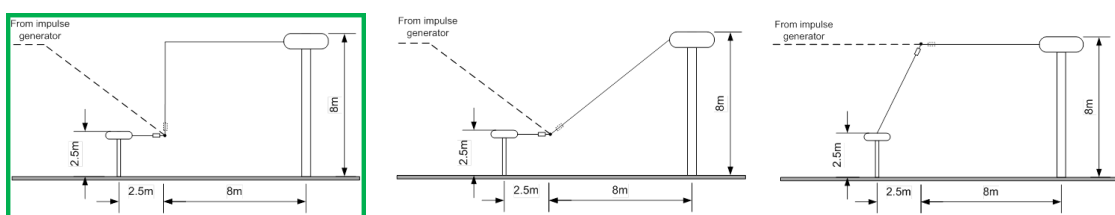


Figure 12: Side view of three measurement geometries.

Input loop size

For studies of input loop size, the step generator was placed on the divider height, and it was suspended in air with low inductance ground connection to the floor. Figure 13 shows the arrangement for loop size changes. The distance to the step generator was varied and the results are shown in Figure 14. Inductance in the circuit increases oscillations and the response time in the HV circuit. There is also a correlation between the T1 error and the rise time of the divider, apparent by the difference in the front time error for short and long front times. The effect on the scale factor of the loop size is below 1 %. Figure 15 shows the measured front time error as a function of damped front oscillation amplitude.

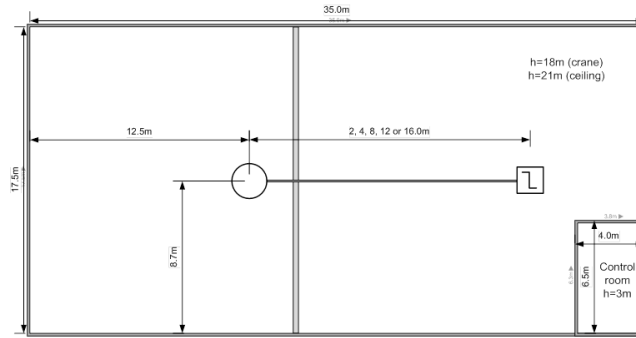


Figure 13: Loop size variations by moving the step generator. Top view of the HV hall.

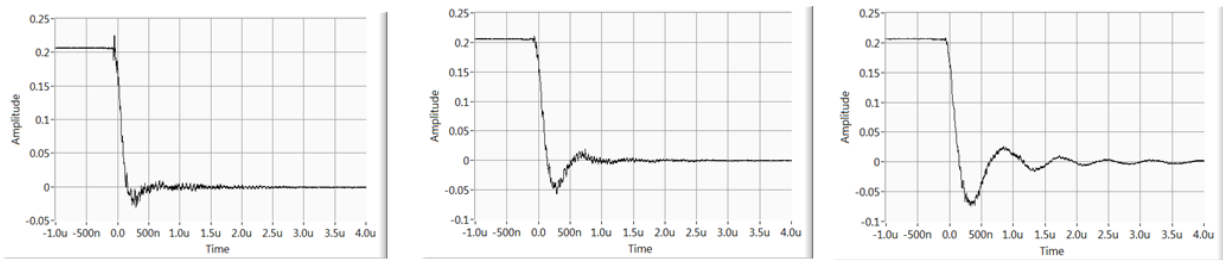


Figure 14: Step response when varying the loop size from 2, to 8 and 16 m (right to left).

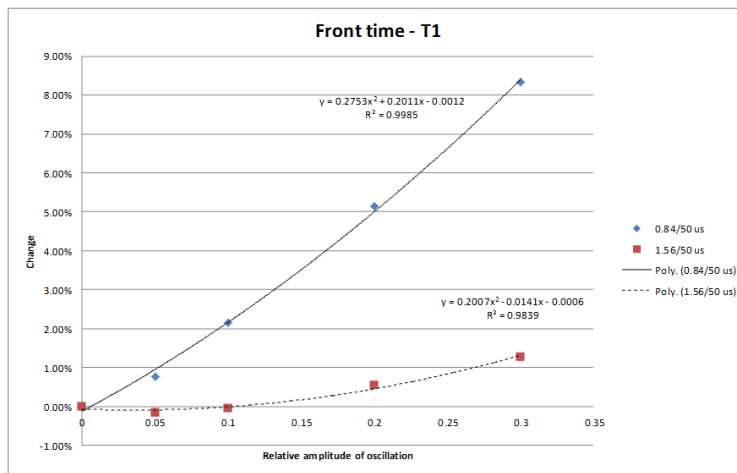


Figure 15: T1 error as a function of amplitude of damped front oscillations for two different front times.

Proximity effect

A study of proximity effects was conducted by varying the distance from the divider to a grounded wall as shown in Figure 16, where the step response generator is placed at the same height with the corona ring of the divider.

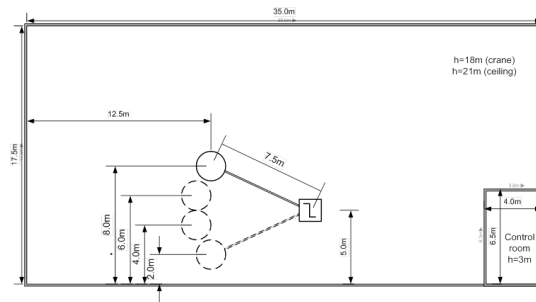


Figure 16: Arrangement for proximity effect study. Top view of the HV hall.

There is a small variation (< 2 %) in the T1 error as a function of distance to the wall. There is also a difference in T1 errors between short and long front times probably correlated to the response time as in the loop size variation. The effect on the scale factor of the proximity is below 2 %

Convolution

After performing step response measurements on the divider, the response is convolved with predefined wave shapes (0.84/50 μs) as defined in IEC 60060-2:2010 in order to determine divider error contributions. Comparison with HV measurements in this study shows deviations, especially for short front times of 0.84 μs, most probably due to oscillations on the front, which to date are not included in the standard. Our experience is that if the front is without such oscillation the agreement is very good.

4.1.4.3 Intercomparison up to 2.6 MV

An overview of the UHV comparison measurement results summarising the results between 9 dividers from three HV sessions is shown Figure 17. The agreement between the peak values is very good at partner ABB (formally STRI; yellow lines). This can be seen as a four step scale factor product (yellow circles). In such a four step scale factor intercomparison, claiming an expanded uncertainty of 0.5 % (new CMC target) one should end up with an error lower than  $\sqrt{4} \cdot 0.5 \% = 1 \%$ . The results as reflected by the circle product error (yellow circles) indicate well below 1 %.

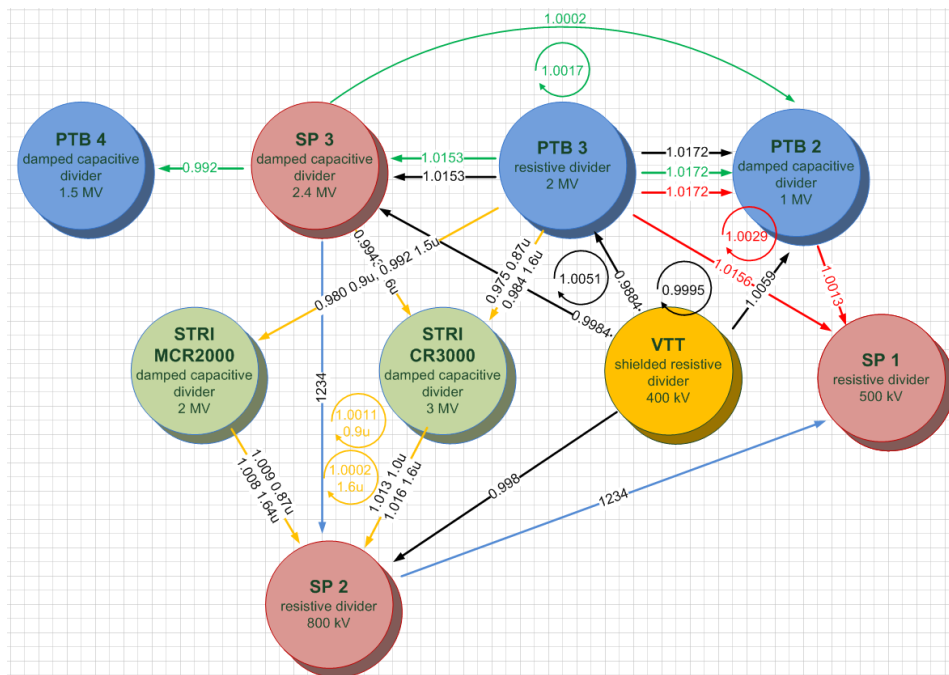


Figure 17 Intercomparison of scale factors between 9 dividers. Values on arrows show the results of one-to-one comparisons, and values within circles show the results of closing the triangles or squares.

#### 4.1.4.4 Observations

Comparisons of a UHV divider (CR3000) HV calibration versus convolution of the step response by a standard pulse shape showed non-satisfactory deviations in prediction of the error of front time T1. We believe that the HV calibrations suffered from the influence of oscillations on the front. Such oscillations are typically only detected by resistive dividers (up to 800 kV class) having faster response than the UHV dividers. It is thought that this difference leads to anomalous results in the determination of the front time T1. The oscillations are typically observed for front times below 1  $\mu\text{s}$ , e.g. when measuring the 0.84/60  $\mu\text{s}$  impulse, but have also been observed at longer front times. The origin is unknown, but one theory is that having slightly misadjusted sphere gaps in the impulse generator combined with a selection of front resistors (damping) might give this ringing.

Theoretical evaluations of standard wave shapes were undertaken for the case of superimposed damped oscillations on the front. The frequency was chosen was approx. 5 MHz and with varying amplitude (Figure 18). The oscillation shifts the 30 % point on the front but not the 90 % point, both which are used in the evaluation of T1 in the standard IEC 60060-2:2010. The filtering introduced by evaluation of the test voltage function defined in the standard, mitigates the shifting of the 30 % point to some extent, but is not fully satisfactory. The “filtering” due to the slower response of the UHV divider seems to deviate from the action of the digital filtering for the test voltage function. The implications are not clear at this time but should be considered by the HV community.

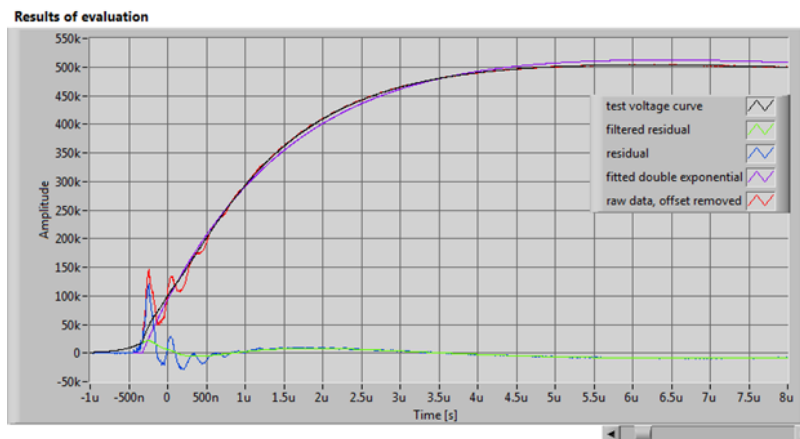


Figure 18: Curve analysis of an impulse with front oscillation with a relative amplitude of 10%.

#### 4.1.4.5 Conclusions for the UHV divider calibration

The comparisons propose that with careful calibration and consideration of proximity and loop effects, it is possible to reach uncertainty close to 1 % for the measurement of test voltage value. However, it is difficult to estimate the errors and uncertainties related with time parameter measurement. In particular, the systematic errors in front time measurement are in many cases several tens of per cent, due to the slow response time resulting from the large size of the divider and test setup. The electromagnetic field travels from the top of the divider to its bottom in light speed, and it takes about 10 ns. The rise time of the impulse to be measured is less than two orders of magnitude larger, below 1  $\mu\text{s}$ .

## 4.2 Objective 2, Very fast transients

### 4.2.1 Measurement of fast transients during puncture testing

#### 4.2.1.1 Rationale

During service, line insulators are stressed by lightning over-voltages. The amplitude and the steepness of the actual stress are influenced both by rated line voltage and by the number of insulators in case of insulator strings. The present version of the puncture testing standard is based on the work performed in CIGRE Task Force 33.07.01 in the late 80's. IEC 61211 describes the methods and requirement for puncture test on ceramic and glass insulators.

Comparisons between tests and field experience have highlighted that impulse voltage puncture tests on insulators units are effective in reducing the risk of failure in service, highlighting design problems or fabrication defects. In puncture test, a fast-rising voltage is applied to the disk insulator and should not lead to puncture of the solid insulation, but to an external flashover.

During puncture testing the test voltage steepness is increased, until it reaches 2.0 to 2.8 times (depending on the insulator type) of the average LI 50 % flashover voltage. In the case of puncture tests, test voltages may reach 500 kV with a resulting time to peak down to 200 ns. This sets the requirements for the measuring system, which are difficult to fulfil using a system designed for LI testing. The main practical difficulty with the LI divider is its large size (height), which prevents building a compact test setup.

In this project a compact divider was designed to address this issue. Calibration methods were reviewed and then applied to the new compact divider.

#### 4.2.1.2 Divider design

The designed divider is based on ceramic resistors. The HV arm consists of a stack of 26 units of 200  $\Omega$  ceramic disk resistors mounted on a threaded fibreglass rod. The low voltage arm is housed in a cylindrical brass container and it is a 5  $\Omega$  ceramic disk resistor, similar to the ones in HV arm. A 45  $\Omega$  matching resistor is used, and the signal output is via an N-connector. A spherical HV electrode is used to reduce the field strength on the top of the divider, and there is a guard ring at the bottom of the divider to guide flashovers to ground.

The coaxial 50  $\Omega$  cable has 100 % shield coverage to reduce interference pick-up, and it feeds the signal to wideband (3 GHz) pulse attenuator with 34 dB attenuation. The total attenuation is adjusted to so that it can be connected to 50  $\Omega$  input of a wideband oscilloscope. A schematic diagram of the divider is shown in Figure 19.

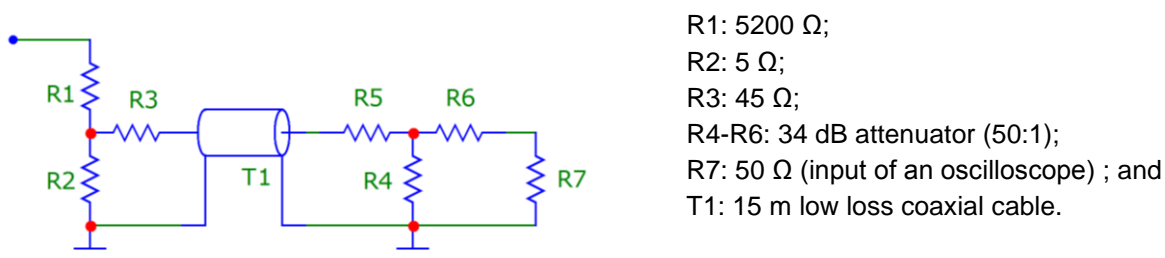


Figure 19: Schematic diagram of the divider and the component values.

These values lead to overall nominal scale factor of approximately 105 000:1. This leads to maximum of approx. 6 V at the oscilloscope input, when 600 kV is applied to the divider input. Most wideband oscilloscopes can typically handle this, when used with 50  $\Omega$  input setting.

#### 4.2.1.3 Characterisation

The step response of the divider was measured in a setup shown in Figure 20, left. The setup is similar to that of actual puncture tests. A step generator based on a mercury-wetted relay is used to create approx. 200 V step with a rise-time of approx. 1 ns. Approximately 300 steps (approx. 2 mV at the oscilloscope input) were averaged to obtain the response shown in Figure 20, right. The response also shows high frequency oscillations, which are dependent on the changes in the setup.

One of the drawbacks of the ceramic resistors is their voltage non-linearity. The voltage non-linearity of the divider was measured against a calibrated LI voltage measuring system. The result of a calibration up to 450 kV using standard LI is shown in Figure 21. In higher voltages, the probability for external flashover with full LI increases along the short divider. The measured linear voltage dependence is typical for ceramic resistors.

The puncture testing standard requires that the scale factor of the divider should be known with an uncertainty of no more than 2 % ( $k = 2$ ). To fulfil this requirement, the non-linearity of the divider has to be corrected, e.g. by software. The measured temperature dependence of the divider scale factor is  $-0.06 \text{ \%}/\text{K}$ .

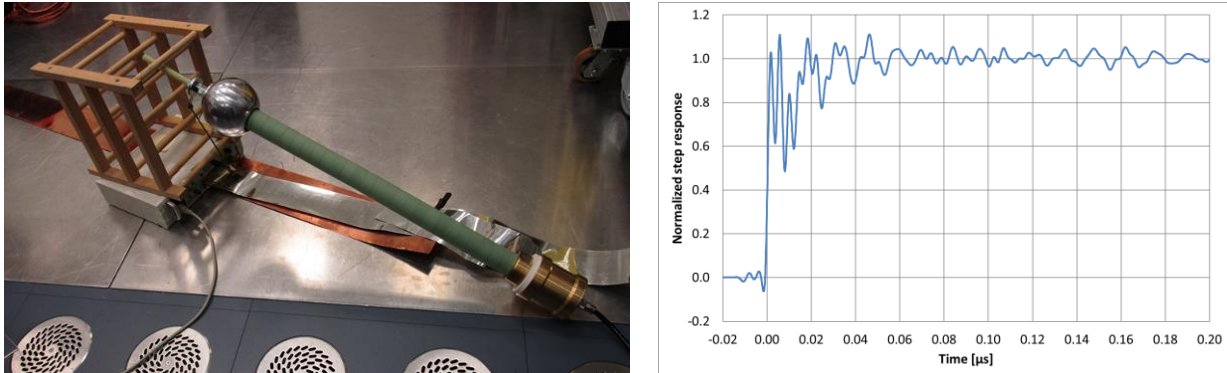


Figure 20: Left: Step response measurement setup. The step generator is under the wooden structure used to support the divider. Right: Step response measured using an oscilloscope with 250 MHz bandwidth and 10 GS/s sampling rate.

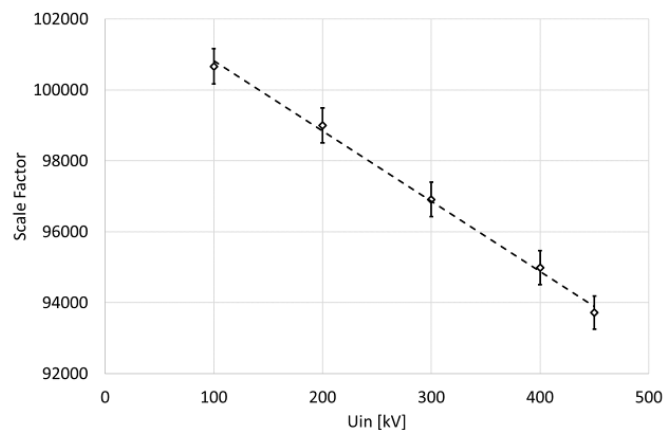


Figure 21: Full LI voltage calibration showing the voltage non-linearity.

#### 4.2.1.4 Performance

A compact puncture test setup is shown in Figure 22 without the impulse voltage generator. The divider is connected directly across the test object on its holder. The loop formed by the ground plate, test object and divider is kept small. In addition, the distance from the peaking gap to the test object is short. Typical impulse waveforms measured with the divider in compact setup are shown in Figure 23.



Figure 22: Compact puncture test setup. The insulator under test is upside down on the ground plane, and the divider input is connected directly to it. The spark gap on the top of the setup is needed for generation of the fast-rising test voltage.

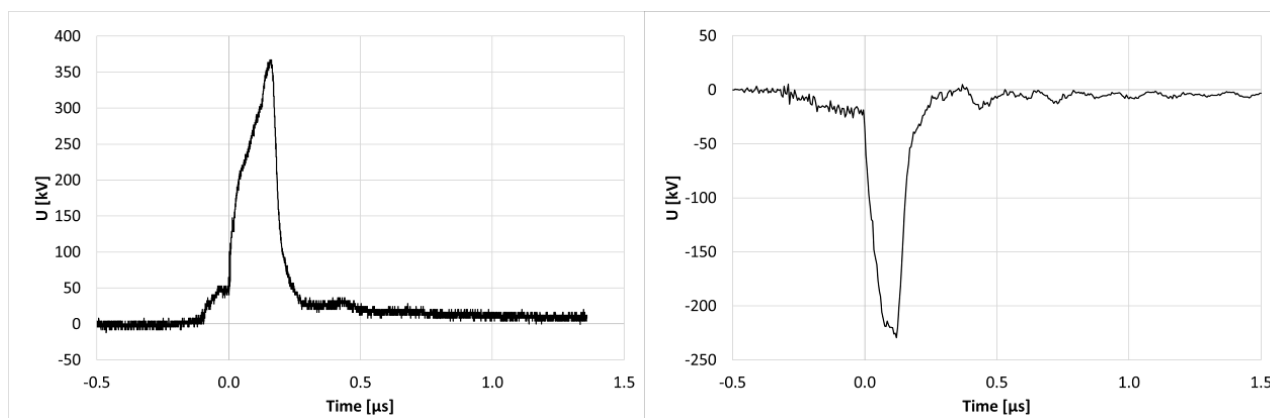


Figure 23: Puncture test waveforms measured in two test laboratories using the new divider.

#### 4.2.1.5 Conclusions

The objectives have been met by the design, construction and performance of a divider for puncture testing together with proof of performance based on the developed calibration methodology. The design of the divider is based on using ceramic disk resistors. The divider has a nominal maximum voltage of 600 kV for measurement of transients shorter than 0.5  $\mu$ s, and the nominal full lighting impulse voltage withstand is 400 kV. The measured rise-time of the complete divider is less than 2 ns.

The divider is designed for compact setup, and for connection to wideband 50  $\Omega$  recording instruments. The divider shows voltage non-linearity, which has to be numerically corrected for accurate measurement results.

Several dividers have since been manufactured, both for project partners VTT, RISE and ABB (formerly STRI) and for external testing laboratory Verescence La Granja (Spanish insulator manufacturer).

## 4.2.2 Generation and measurement of fast current steps

### 4.2.2.1 *Rationale*

High impulse current is required not only for testing equipment such as fuses and surge arresters, but also for technical applications e.g. lasers, thermonuclear fusion, and plasma devices. In technical and scientific fields, it is necessary to determine the waveform and amplitude of a rapidly varying high current. The range of the current amplitude may range from few amperes to hundreds of kiloamperes while the rise-time of these currents can vary from microseconds to few nanoseconds. The sensors or measuring devices should be capable of measuring the signal over a wide frequency range. The sensors commonly used include resistive shunts, magnetic potentiometers or probes, Faraday and the Hall effect devices. The aim of this part of the project's work was to develop a traceable infrastructure and calibration and measurement techniques for very fast current impulses, and to improve the present test procedures and measurement capabilities.

International standard IEC 62475:2010, *High-current test techniques - Definitions for test currents and test systems*, sets the requirements for impulse current measuring systems. A simple version of a coaxial cable-based generator for testing dynamic behaviour of impulse current shunts is described in its Annex C (see Figure 24).

### 4.2.2.2 *Step Current Generation*

The cable with characteristic impedance  $Z$  is charged to voltage  $U_0$  through resistor  $R_1$  (See Figure 24). The cable is discharged to shunt (or coil) using switch  $S$ .  $L$  is the inductance of the circuit connected to the cable. When the spark gap switch  $S$  is closed, a steep wave of current enters the coaxial cable. This wave is reflected from the open end of the cable, and it travels back from the open end to the entry point of the cable with the same amplitude and polarity.

For  $Z_a=Z$ , the current would then die out at the terminating load impedance  $Z_a$  after twice the cable travel time. However, in our case for  $Z_a<<Z$ , the reflection phenomenon happens again at the load, now with polarity reversal. A recorded curve is shown in Figure 24.

The duration of each current step generated depends upon the cable length  $l$ . The cable return travel time is

$$t = 2l / v ,$$

where  $v = 1/\sqrt{L_0C_0}$ , and  $L_0$  and  $C_0$  are the characteristic inductance and capacitance of coaxial cable. Only the first step was used in this project, as the subsequent reflected waves are influenced by attenuation of the cable, imperfect reflections at the load end and, in the case of spark gap switch, losses due to gap arc extinction and re-ignition at each zero crossing.

The current delivered by the generator depends on the charging voltage, characteristic impedance of the cable and load impedance  $R$ :

$$I = \frac{U_0}{(Z + R)} .$$

The relation between the rise-time  $\tau$  of generated current step and total inductance  $L$  of circuit components including spark gap and connection is given by:

$$\tau = \frac{L}{Z + R} .$$

Therefore, when  $R \ll Z$ , the rise-time is limited by the  $L/Z$  time constant of the circuit. In order to reduce the rise-time, the circuit was kept coaxial to minimise its inductance. The inductance, and thus the rise-time, is affected by the type of switch and type of medium in case of spark gap. For the rise-times below approx. 10 ns, it suggests that the inductance of spark channel dominates the switch performance.

In several hundred meters long cables the resistances of the inner and outer conductors cannot be neglected. It causes phenomenon called droop, which describes that the current will decrease slightly as the impulse gets longer. In the beginning, the wave impedance only affects the amplitude. But when the wave propagates further the voltage drop across the conductor's resistance gets higher and therefore the peak current decreases. The resistance of 100 m long RG-213 is about 1  $\Omega$  for the inner and outer conductor, therefore the amplitude will be reduced by 4 % within this 50  $\Omega$  cable.

Two different setups were built by the project, one at VTT and another one at PTB. Key data for the setups are listed in Table 6. The charging voltage is limited to 5 kV by the characteristics of the N-connector used in both setups.

**Table 6 Step current cable generator setups**

	PTB	VTT
Cable type	RG-213	1/2" Heliax
Cable length	500 m	110 m
Step duration	5 μs	1 μs
Charging resistor	50 kΩ	30 MΩ
Maximum charging voltage	5 kV	5 kV
Maximum current	100 A	100 A

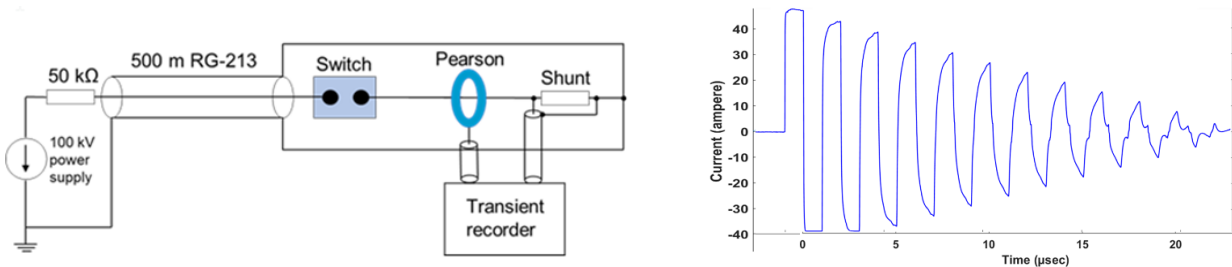


Figure 24. Coaxial cable based current step generator for testing impulse current shunts and its output waveform. The component values are for the PTB setup.

Argon, air and SF<sub>6</sub> filled spark gaps and reed relays were used for switching. Effort was taken to keep the circuits as compact as possible, and to match them to 50 Ω impedance of coaxial cable as much as possible. Two different spark gap designs are shown in Figure 25. Both use 50 Ω N-connectors, and the VTT one has an additional coaxial return path for the current.

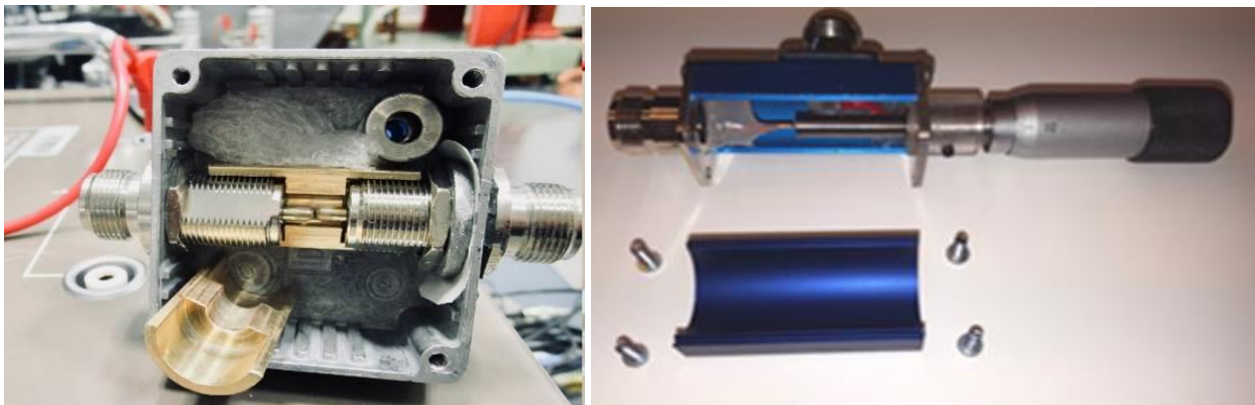


Figure 25. Adjustable coaxial spark gaps. VTT design (left) has brass electrodes, and additional ground path next to the gap. It must be opened for adjustment. PTB design (right) has tungsten carbide tips, and it can be adjusted using a micrometer gauge attached to the enclosure.

The reed relay switch used by PTB is shown in Figure 26. DAT 71210 type relay is placed in a CNC milled housing. The input and output connectors are also N-Type except for the BNC-type trigger input for the coil.



Figure 26. PTB's reed relay box.

4.2.2.3 Measurement Setup

Due to common mode grounding problems, two shunts cannot be directly compared against each other. However, it is possible to compare the response of a shunt with a current sensing coil as shown in Figure 27. Short coaxial cables matched to 50 Ω are used for transferring the signal from sensors to an oscilloscope. The setup is on an aluminium plate, with cables grounded on both ends using wide conductors. During the testing, the oscilloscopes were remotely controlled via optical fibres. The tested current sensors are listed in Table 7.

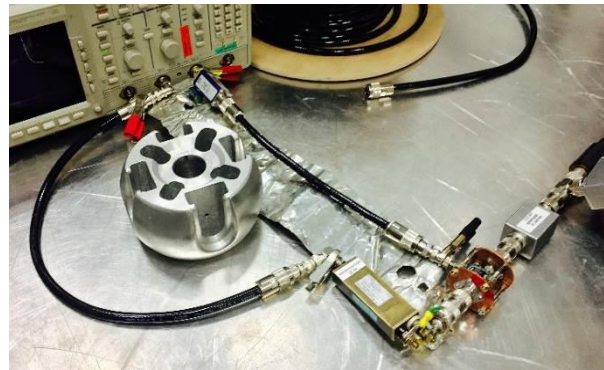
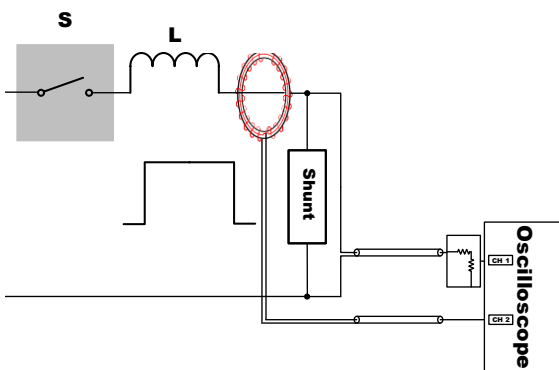


Figure 27. Left: Circuit diagram for measurement of current step using shunt, coil, attenuator and oscilloscope. S and L representing spark gap and total inductance of circuit, respectively. Right: starting from the right: end of the coaxial cable, box with spark gap, a current sensing coil in coaxial cage and a shunt. The outputs of the coil and the shunt are connected with short coaxial cables to the oscilloscope.

Table 7 Tested current sensors and their main specifications.

Sensor	Manufacturer	Model	Nominal sensitivity	Nominal rise-time
Coil (P2)	Pearson Electronics	2877	1 V/A	2 ns
Shunt (S1)	T&M Research Products	W-1T-5-1STUD	0.5 Ω	1 ns
Shunt (S2)	T&M Research Products	W-1-1-1STUD	0.1 Ω	1 ns
Shunt (S3)	T&M Research Products	W-1-01C-2FC	0.01 Ω	0.45 ns
Shunt (SH)	HILO-TEST	ISM 5P/50	0.05 Ω	1.8 ns
Shunt (SH2)	HILO-TEST	ISM100	0.001 Ω	1.8 ns
Shunt (SH3)	HILO-TEST	ISM 5P/10	0.01 Ω	1.8 ns
Coil (P3)	AMS Technologies	CT-1.0-BNC	1 V/A	0.7 ns

4.2.2.4 Results and Discussion

An overview of the measured rise-times with different gaps is shown in Figure 28. Different sensors and oscilloscopes were used for the measurements, but the results shown are in most cases not limited by the characteristics of the measurement system. A typical measured response is shown in Figure 29.

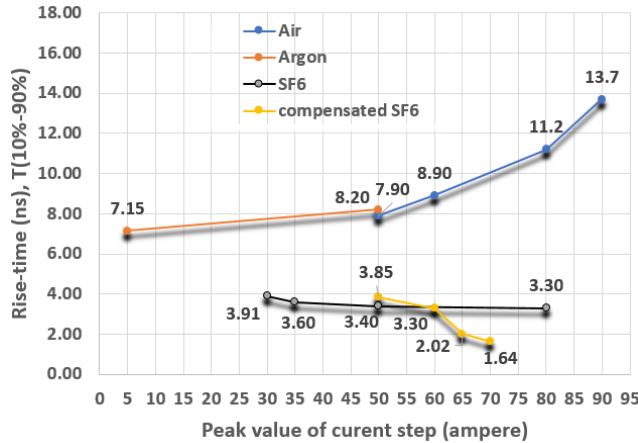


Figure 28. Relation of rise-time with various spark gaps and step current values.

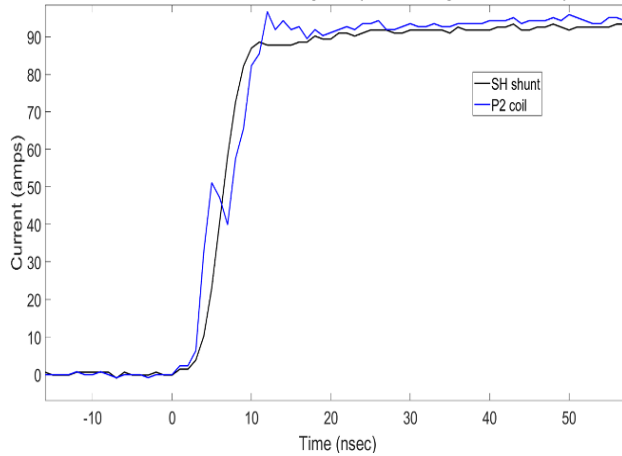


Figure 29. 90A current step measured by a shunt and a fast current sensor.

The PTB reed relay generator shows an almost constant rise-time of 2 ns up to 70 A (3.5 kV). From these measurements it is evident, that with increasing spark gap distance, the rise-time will get longer. In order to achieve faster rise-times at higher amplitudes, it is necessary to reduce the spark gap distance by either increasing the pressure or using a better insulating gas, or even both.

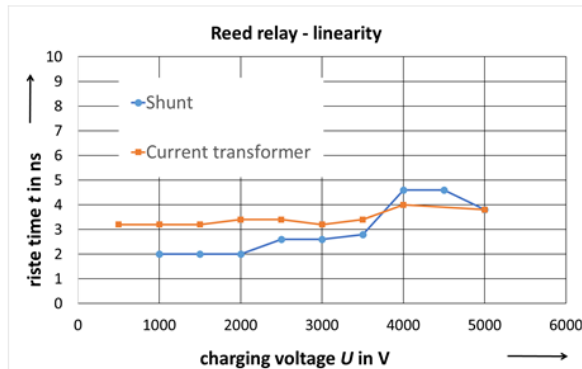


Figure 30. Rise-times obtained using the reed relay as function of charging voltage. Shunt SH2 and coil P3.

Shunt responses were compared so that one shunt was used with the coil at a time in each test session. The ratio of the currents measured by shunt and coil is shown for different combinations in Figure 31.

S1 shunt was considered as a reference for the analysis below. The impulse ratios of the other shunts were calibrated for time epoch from 750 ns to 900 ns, using the DC resistance of S1 shunt as reference.

Typical uncertainty for calibration of the impulse scale factor of a shunt at 1  $\mu$ s after onset of the step was 0.5 %. The differences between DC and impulse scale factors of the tested shunts ranged from 0.3 % to 6 %.

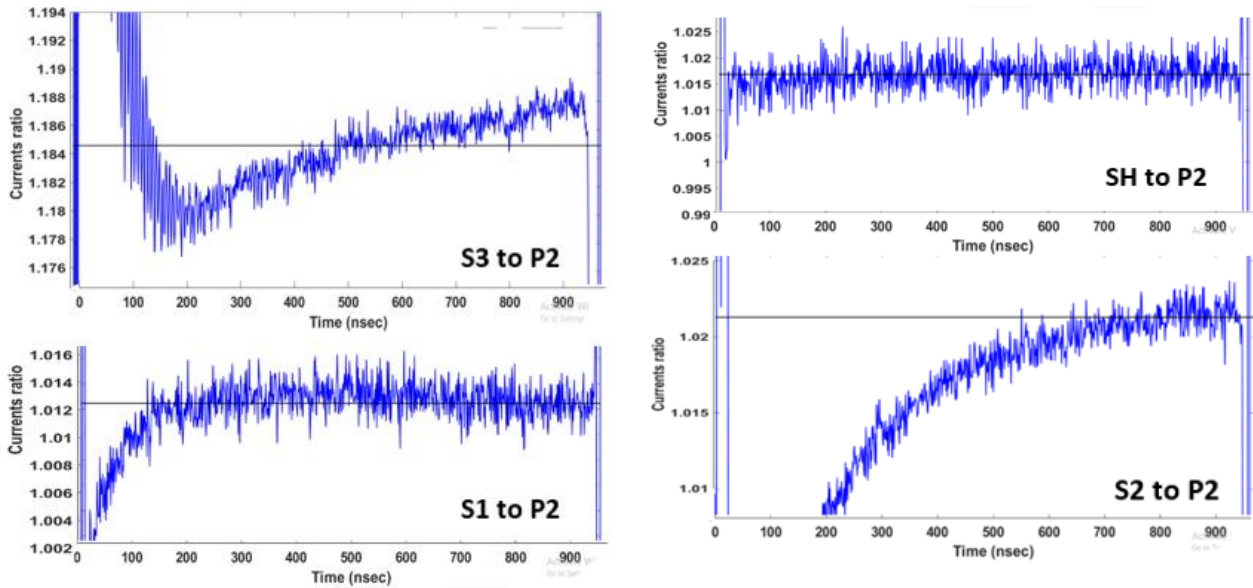


Figure 31. Dynamic performance of (SX), measured by coil (P2) as reference. Vertical scale is un-calibrated.

#### 4.2.2.5 Conclusions

The objective has been met by development of a coaxial cable current step generator, which produces well-defined, rectangular, fast and steep steps of peak value up to 100 A with rise-time less than 5 ns. The duration of the stable current is about 1  $\mu$ s. The generator has been successfully used in VTT’s laboratory for current step generation.

Step current measurements were performed for impulse shunts, using a fast current sensing coil as transfer reference. Three out of the four tested shunts agreed within 1 % after approx. 800 ns from the onset of the step current. Even though all tested shunts claim rise-time below 2 ns, they showed different settling times to final value. Verification of the actual rise-time appeared to be quite difficult. In addition to the characteristics of the switching element, the geometry of the circuit has a significant effect on the measurement.

The length of the cable needed, limits the applicability of the method. For example, about two kilometers of cable would be needed to cover the entire epoch of a standard 8/20  $\mu$ s impulse.

### 4.3 Objective 3, Losses of power transformers, reactors and capacitors

#### 4.3.1 Loss measurement on power transformers

The challenge for power transformer manufacturers is to unambiguously prove that their products comply with the new efficiency requirements of the Ecodesign Directive. To this end, the losses of their products are tested using power TLM systems that must have an accuracy of 5 % or better in their loss measurements. Figure 32 shows a typical schematic of a TLM system used for load loss measurements of power transformers. The actual quantity measured by TLM systems is active (loss) power:

$$P_{loss} = V I \cos(\varphi)$$

Tests are performed at HV and currents, so voltage and current transformers (VTs and CTs) are used for scaling these test signals down to levels that can be handled by a wattmeter (WM) (Figure 32).

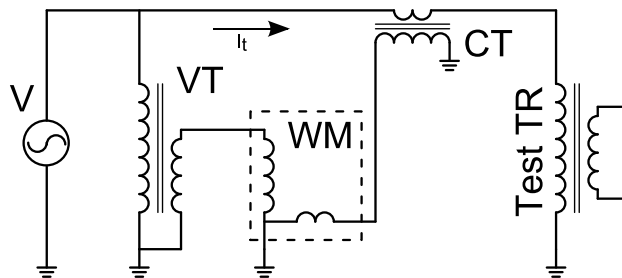


Figure 32: Schematic of a typical industrial setup for loss measurements of power transformers.

The main challenge in transformer loss measurements lies in the measurement of active power under conditions where the transformer losses are low. Here the current is approximately 90° out of phase in respect to the applied voltage, corresponding to a power factor close to zero. The close-to-90° phase shift means that the active power is approaching very small values (low loss), which still need to be measured at an accuracy of 5 % according to the new Ecodesign Directive regulations. This puts very stringent requirements on the phase accuracies of the VTs, CTs, and WM of the TLM system. TLM systems have to be calibrated on-site in the test facility due to their size and weight, and to have minimum down-time. So far, the calibration of TLM systems has been performed via calibration of its individual components. However, combining the results of the individual calibrations into a total TLM accuracy is not easy. More importantly, this method is limited in the achievable accuracy for the total TLM system and does not reveal any system-related errors.

Therefore, in this project, two reference setups have been developed for the calibration of industrial TLM systems as a whole. Such a whole system calibration can reach better overall accuracy and moreover includes all possible systematic error terms. A further significant advantage is that the calibration applies actual (phantom) loss power to the TLM system and thus can be performed for a series of phase angles between voltage and current, which corresponds to those in actual transformer loss measurements. Two complementary approaches were developed by the project for TLMS system calibration:

- 1) The PTB reference setup uses parallel generation of voltage and current test signals.
- 2) The VSL reference setup generates the test current via a feedback loop that maintains a constant phase of the current with respect to the applied HV. This setup can also be used on-site to calibrate TLM systems in the test halls of power transformer manufacturers.

##### 4.3.1.1 Phantom power source using simultaneous generation

The PTB high-power measurement standard is designed to offer a suitable phantom power generation of sufficiently high stability for voltages up to 220 kV /  $\sqrt{3}$  and currents from several amperes up to 2 kA. In order to achieve the desired accuracy of 50  $\mu$ W/VA, well below 100  $\mu$ W / VA (class 0.01) at all power factors from 0 ind. To 1, components are required with small phase errors, and traceable to primary standards.

Therefore, the modular setup uses one or several PTB standard VTs of the error class 0.02 chosen for the required voltage range, one standard CT of the error class 0.002 with current ranges from 5 A to 5 kA, and a commercial digital power comparator (DPC) of the error class 0.01. The DPC is self-synchronising to the measured fundamental frequency, so that any frequency between 45 Hz to 65 Hz can be measured, without degradation of its accuracy i.e. due to leakage effects of the internal measurement algorithm (see Figure 33).

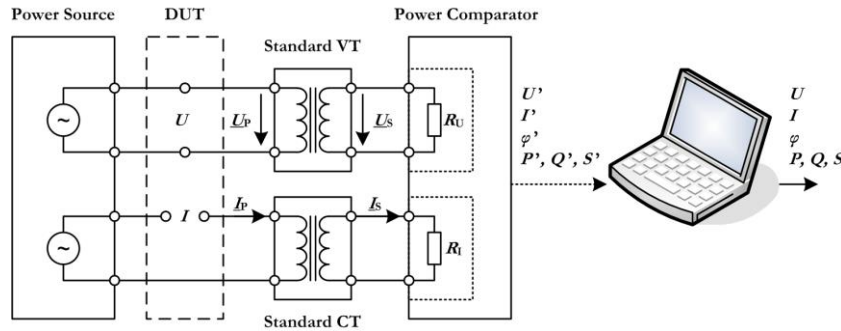


Figure 33 PTB HV power standard. The device under test (DUT) is connected to  $U_P$  and  $I_P$ .

A phantom power source separately provides the required HV and high current at a programmable phase angle. The generated voltage  $U_P$  and current  $I_P$  is fed to the VT and CT of the power standard and to the DUT. An important feature of the power standard is its capability to generate the required test voltages and test currents at any phase angle and, thereby, the active AC power. The VT and CT with their selected voltage ratio  $K_{nu}$  and current ratio  $K_{ni}$  transform the voltage  $U_P$  and current  $I_P$  into the precise secondary voltage  $U_S$  and the secondary current  $I_S$ , respectively, which are connected to the DPC afterwards. The DPC measures the relevant quantities at the secondary of the instrument transformers. A computer (PC) with dedicated software controls the DPC and reads the measured voltage  $U'$ , the current  $I'$ , the corresponding phase angle  $\varphi'$ , and the active power  $P'$  of the DPC. Subsequently, the PC calculates from these results the respective power quantities at the primary of the instrument transformers using their transformer ratios. Dedicated correction algorithms correct for the systematic errors of the components (DPC, VT, CT) and lead to a conservatively estimated measurement uncertainty in the order of  $40 \mu\text{W} / \text{VA}$  of the active power for voltages up to  $220 \text{ kV} / \sqrt{3}$  and up to  $2 \text{ kA}$  at any power factor. The standard will be used for calibrating reference measuring systems of accredited laboratories offering calibration service for calibrating industrial TLM systems or for manufacturers of TLM systems.

Figure 34 shows the realisation of the power source. A programmable two-channel voltage generator with 16 Bit resolution generates two sinusoidal voltages  $U_U$  and  $U_I$  with low distortion ( $< 0.01\%$ ), high stability ( $10^{-6}/\text{h}$ ) and any phase angle  $\varphi$  within  $\pm 180^\circ$  and a resolution of  $0.001^\circ$ . The frequency  $f$  of the source can be adjusted arbitrarily. To allow a power line synchronised generation of the generator or to synchronise it to an existing HV path (e.g. on-site) a PLL circuit is optionally used to clock the generator with  $2048 \times f$ .

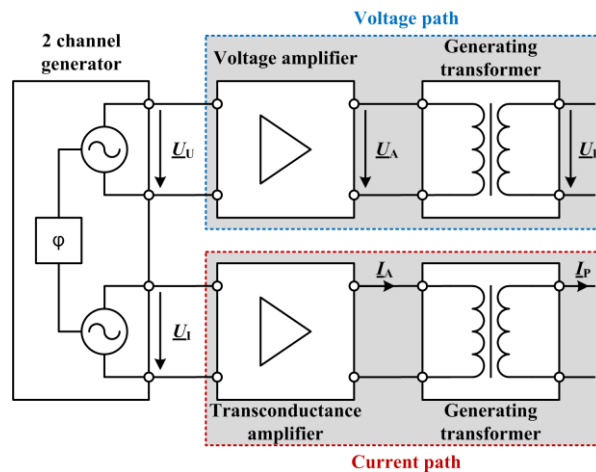


Figure 34. Phantom power source of the high-power standard. The generated test voltage  $U_p$  and test current  $I_p$  is connected both to the reference measurement system and to the DUT (not shown).

To achieve high signal fidelity, the voltage amplifier (UA) and the transconductance amplifier (TA) are analogue high-power amplifiers with a bandwidth of  $15 \text{ kHz}$ . The generated voltage  $U_A$  and the current  $I_A$  of UA and TA are fed to the primary windings of the HV and high current generation transformers. Their secondary windings provide the required test voltage  $U_P$  and test current  $I_P$ . The generation transformers offer several rated outputs from  $1 \text{ kV}$  to  $150 \text{ kV}$  and  $5 \text{ A}$  to  $2 \text{ kA}$ , respectively. In several stability tests of the power source

at different voltage and current levels, a low noise of less than 10 ppm was seen, and drifts were of the order of 50 – 100 ppm/h. This is more than sufficient for the envisaged application.

This source is suitable for stable calibration conditions, as the typical time window for one test point is roughly 30 s during a calibration. Several measurements based on 20 single readings within a time window of 25 s confirmed, that the standard deviation is in the order of below 2 ppm for voltage and current, and in the order of below 3 ppm for active, reactive and apparent power. The associated Type A uncertainty is even lower. The distortion of the test current is below 0.05 % in all ranges of the current generation transformers, while the generated test voltage exhibits a THD of 0.2 % in the 75 kV range and 0.8 % in the 150 kV range.

4.3.1.2 Phantom power source using feedback loop

A crucial element in system calibrations of industrial TLM systems is the availability of test voltage and current signals with adjustable phase close to 90°, that is a power factor near to zero (low losses), in order to apply a known and stable loss or reference power to the TLM system. Similar to the approach of PTB, a phantom technique, separating the current and voltage circuits, is used by VSL to simulate different losses to the TLM system. However, in the reference system developed by VSL, digital signal processing is used to maintain the phase relation between the voltage (up to 100 kV) and the generated current (up to 2000 A) applied to the TLM system (see Figure 35). In principle the relation between current and voltage can mimic any impedance but for the purpose of TLM calibrations an inductor needs to be simulated.

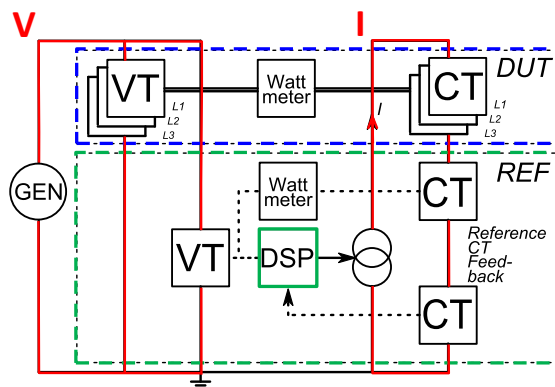


Figure 35. A typical TLM measurement system consisting of a three-phase WM and VT's and CT's. The reference system is placed in parallel with the TLM's VT's and series for the TLM's CT's creating a phantom power. The DSP calculates the needed current signal to simulate different load conditions.

The great benefit of using DSP instead of an analogue approach, is that it allows flexibility and easy automation while at the same time still reaching excellent accuracies. The DSP of the VSL reference system is based completely on adjustable digital filters which define the relation between voltage and current (input and output of the DSP, as shown in Figure 35). First a 90° copy of the voltage input signal is made by means of a first order integrator. By selecting the proper combination of I and Q (see Figure 36), the right mix of in-phase and quadrature signals are added, so that any phase shift between input and output of the DSP can be generated. A second DSP measures the actual phase shift between the input voltage and the applied current and subsequently adjusts I and Q in the first DSP until the measured phase matches the set-point.

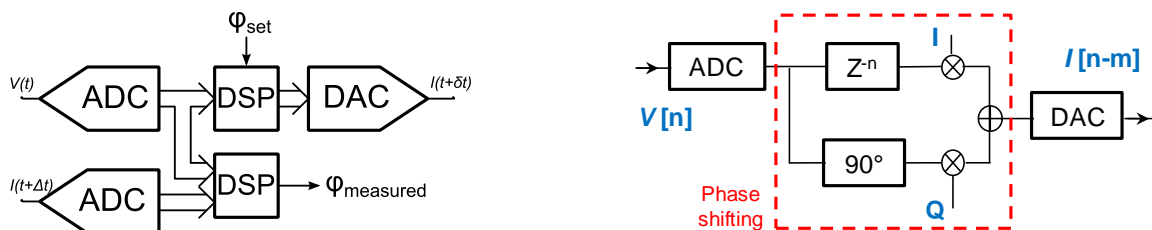


Figure 36: Left: Phase shifting of the measured signal is done with the top DSP and the calculation of the phase is done by the bottom DSP. Right: the workings of the top DSP for phase shifting. The original signal  $V_n$  is phase shifted by 90° and is summed with the original signal in the right ratio of I and Q

The current has to follow variations in voltage as fast as possible in order to maintain a stable phase angle between voltage and current under all actual test conditions. The biggest challenge in the overall DSP approach lies in reducing the latency between the input and output signal, which is realised by using fast analog-to-digital converters (ADCs) in the first DSP. Their limited accuracy is compensated by the second DSP that has high-accuracy (but slower) ADCs. The time constant of the control loop is in the order of a few hundred milliseconds, sufficient to compensate phase drifts in applied voltage and drifts due to e.g. warming of the power amplifier. The complete system is transportable and fully automated.

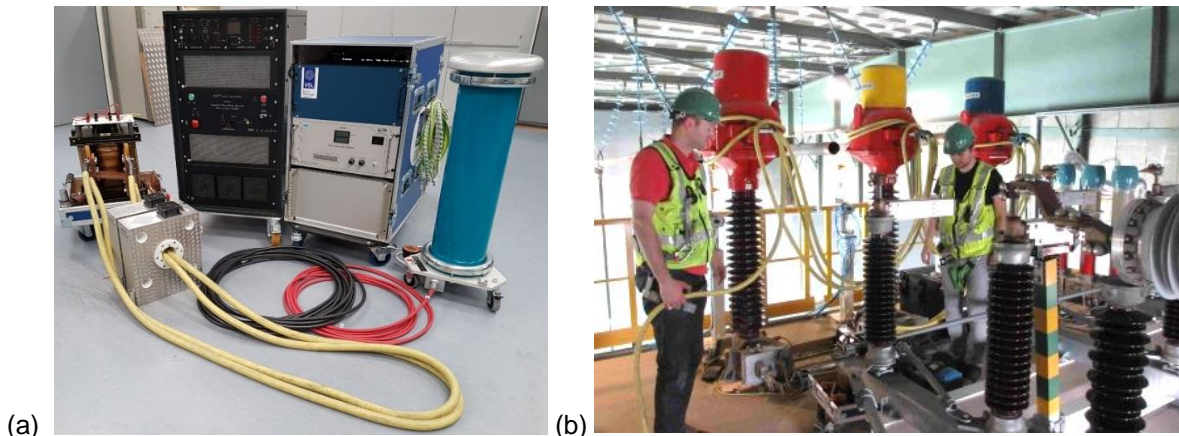


Figure 37 (a) Portable reference system for on-site TLM calibrations. Showing from left to right. Generation transformer, reference CT's, Power Amplifier, DSP and HV divider and capacitor. (b) On-site measurement, showing three VT's and three CT's. The CT's are connected in series with high current cables.

A variety of tests were performed during the development of the set-up and algorithms in the DSP unit. When the HV source is driven by a stable and pure sine wave, the algorithms in the DSP are not very critical for the final feedback loop behaviour, and phase noise levels of around  $5 \mu\text{rad}$  (5 ppm) can be relatively easily achieved. However, in actual on-site TLM system calibrations the HV source is either driven by the mains grid or by a separate generator. This results in significantly larger frequency and phase variations of the applied HV, which makes the selection and parametrisation of the DSP filters and algorithms much more critical. After a long series of algorithm optimisations, better than  $10 \mu\text{rad}$  phase noise levels were achieved for a HV source driven by the mains grid.

Figure 38 shows a typical result achieved after this final improvement. The test is performed at 50 kV, 1000 A, 50 Hz, with the phase angle set to  $\text{PF} = 0.01$ . The result proves the better than  $10 \mu\text{rad}$  phase noise also for HV signals with significantly varying frequency and phase – typical for on-site situations.

To prove the best uncertainty levels achievable by the reference setup, all critical components of the setup were calibrated. All calibrations are performed at both 50 Hz and 60 Hz, the frequencies at which the TLM calibration reference setup is used in practice. Based on these calibrations, for a 50 Hz calibration at  $V = 100 \text{ kV}$ ,  $I = 2000 \text{ A}$  and a  $\text{PF} = 0.01$ , the uncertainty budget is 0.0021 % (21 ppm). As expected, the main uncertainty contribution at this low power factor is from the total correction in phase  $\varphi$ , with the two largest contributions arising from the  $7.5 \mu\text{rad}$  phase uncertainty in the reference power meter calibration and the  $5 \mu\text{rad}$  phase uncertainty in the calibration of the current-comparator-based voltage divider.

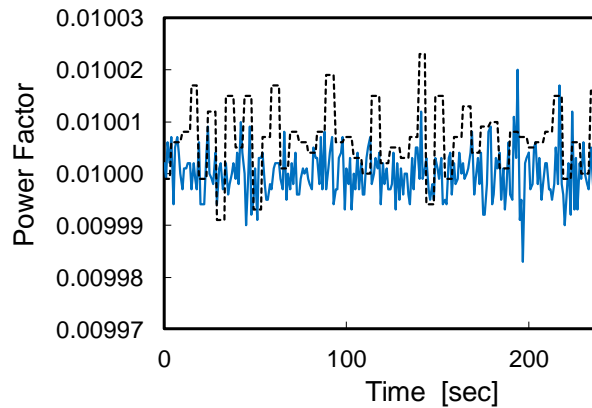


Figure 38 Power factor as function of time for a test at 50 kV, 1000 A, 50 Hz, PF = 0.01. Excellent agreement between the DSP active power measurements and those of the reference power meter: the readings differ only 8  $\mu$ rad which is well within the measurement uncertainty of both reference power meter and DSP system

To solve the problem of accurate power reference generation, TU Delft took another (complementary) approach to VSL, with the goal of comparing real-life performance of the two (i.e. the reference power meter and DSP system). The VSL method involves the digitisation of a proven analogue solution which has the advantage that an operational (analogue) reference exists, and that the risk is reduced. The TU Delft approach involves a direct application of the fundamental theory, and as a result offers possibility of improved controllability and robustness (e.g. a potential to eliminate the influence of harmonic distortion, compensate for delays).

A typical setup for calibration of power transformer (shown Figure 32) can be divided in two distinct parts; the hardware and the software (control) part. Given that VSL provided the hardware setup, with sufficiently accurate components, attention was focused by TU Delft on identifying and selecting a suitable (digital) control algorithm for implementation on the digital controller.

As stated in the requirements, the goal is to generate a current reference signal, with sufficient phase and amplitude accuracy (as defined in the input requirements). This signal is converted from the digital to analogue domain using a digital-to-analogue converter (DAC), amplified (with transconductance amplifier) and injected in the system for calibration. The parameters of this reference signal (phase and amplitude) are derived from a given (on-site) voltage reference, adjusted (attenuated) using appropriate voltage dividers and digitised with a precision ADC. The injected current is monitored with a highly accurate CT, sampled and digitised using another ADC and used in a feedback loop to compensate of instabilities and uncertainties of the components in the system. A high-level block diagram of the proposed control system is shown in Figure 39.

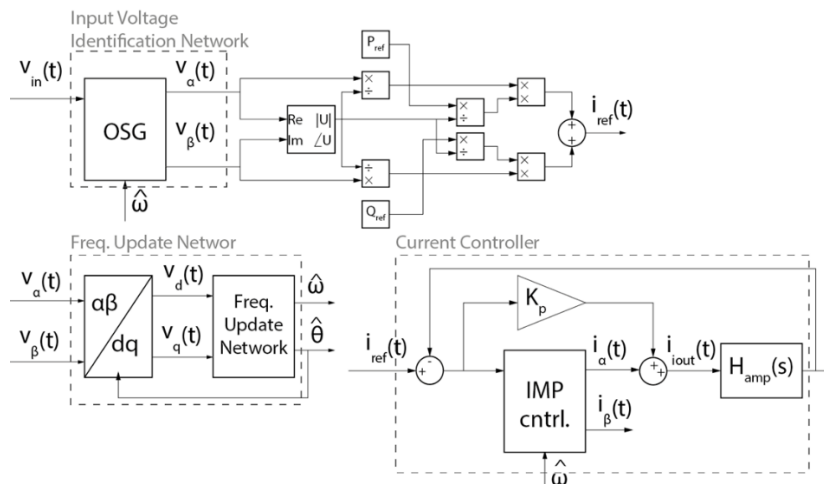


Figure 39. High-level block diagram of the proposed control strategy

To comply with the requirement of 50  $\mu$ rad of phase uncertainty, the target during control design was to have power reference error better than 5% at power factor of 0.001 (almost 10-times better than required). This

gave a sufficient margin to accommodate uncertainties of the other components in the system (e.g. transconductance amplifier, voltage dividers, ADCs and DAC etc.)

The critical part of the control system is identification of the input voltage signal. This is done with subsystems '*Input Voltage Identification Network*' and '*Frequency update network*', as designated in Figure 39. In steady-state, outputs of the first block, signals  $V_\alpha(t)$  and  $V_\beta(t)$ , have the same amplitude and are respectively in phase and in quadrature (phase delayed by  $\pi/2$ ) with respect to the input signal. What this means is that in steady state, the signal  $V_\alpha(t)$  accurately (and without steady-state error) is tracking the input signal. This state is often referred to as a 'locked' state as both signals maintain the same phase and amplitude. However, to reach this 'locked' state, the parameter  $\hat{\omega}$  must be equal (to the permissible error defined by the requirements) to the angular frequency of the input periodic signal. Tracking of  $\hat{\omega}$  is performed with subsystem termed '*Frequency Update Network*'. This is a second-order system, and as such is capable of tracking input sinusoidal signals with zero steady-state error.

To generate the reference current  $i_{ref}(t)$ , given active  $P_{ref}$  and reactive  $Q_{ref}$  power references are divided with the voltage signals  $V_\alpha(t)$  and  $V_\beta(t)$  as shown in Figure 39. This current reference is then used in the final sub-system '*Current Controller*' to generate output current reference. Block  $H_{amp}(s)$  represents a transconductance amplifier (mentioned in the previous chapter) which amplifies the signal from the DAC. Output of transconductance amplifier is fed back in the control system for closed-loop operation.

The high-level block diagram of the proposed controller is relatively common when control of harmonic signals is involved. However, rather unusual decomposition (particularly when it comes to signal identification subsystem – often called phase-locked loop) is something that has arisen while attempting to identify major sources of uncertainties in the control system. In the initial design stages, while surveying state-of-the art solutions for identification of sinusoidal signal, it was observed that majority of the systems proposed in the literature have similar dynamic behavior. Further investigation revealed that, all the systems pertaining to identify period signals must include the model of the sinusoidal signal, designated as an orthogonal signal generator block (OSG) in Figure 39. This is a non-linear system, with  $\hat{\omega}$  figuring as a parameter, which is the unknown angular frequency of the input signal. As such, this subsystem requires a way to estimate this unknown frequency. It is this, the frequency update subsystem, where the most of the phase-locked loop (PLL) algorithms differ. This observation and subsequent decomposition of the phase locked loop system in the two subsystems (one of which stays the same for all PLLs) helped systematically classify PLL systems and is one of the contributions of this project.

Numerical simulations were carried out (using MATLAB/SIMULINK) to tune the parameters of the system and confirm suitability of the proposed model for the target application. The following conclusions can be drawn:

- The system met (and exceeded) all initial requirements (5 % power error at 0.001 power factor).
- The system is capable of operating under conditions where the input signal is relatively instable (both, instable amplitude and frequency), exceeding capabilities of similar state-of-the art analogue systems.
- The control system proved to be very resilient to the presence of harmonics. If a harmonic exceeds the certain level (observed by monitoring an internal error signal), a selective harmonic cancellation can be easily introduced to compensate for it, allowing for even higher presence of harmonics.

This demonstrates the full potential and flexibility of the digital control. By changing only the software, the behaviour of entire system can easily be altered and adapted to a variety of circumstances, unknown at the moment of the system design (something impossible when analogue control is used). All this was enabled by advancements in DSP and Field Programmable Gate Arrays (FPGA) showing that the future of control is in the digital domain.

#### 4.3.1.3 Comparison of approaches

In November 2018 VSL brought their transportable reference system to the PTB premises to perform a comparison between the two complementary systems. During the visit two measurements were performed, according to the main operation modes of the PTB and VSL setups:

1. PTB generates voltage and current, that both VSL and PTB measure.
2. PTB generates voltage and VSL generates current, that both VSL and PTB measure.

In addition to the two measurements above, all 3 main components of the systems were individually compared. This comparison of the reference WM, the CT's and the VT's was planned to give more insight in the origin of any possible deviations between the two systems.

The results of the component comparisons were as follows:

- for power the differences between the PTB and VSL component results were less than 5 ppm in magnitude and around 10  $\mu\text{rad}$  in phase,
- for the CT's an excellent agreement was found between the PTB and VSL component results of better than 3 ppm in ratio error and 3  $\mu\text{rad}$  in phase displacement,
- and for the VT's of the differences between PTB and VSL's component data was around 10 ppm for ratio error and better than 5  $\mu\text{rad}$  in phase displacement.

For TLM calibrations, in particular, the phase is important, therefore these are important and very encouraging results.

Indeed, the system comparison of the complete PTB and VSL reference systems confirmed the good results of the component comparison. For currents in the range of 100 A to 1000 A, the results agree at the level of better than 12  $\mu\text{W}/\text{VA}$ . For higher currents of 1600 A, 1800 A, 2000 A, a slightly higher deviation is found, but all results still agree within 20  $\mu\text{W}/\text{VA}$ . A typical result is given in Figure 40. The 13  $\mu\text{W}/\text{VA}$  deviation of the VSL verification measurement from the other results might be due to instabilities of the reference WM used in the verification.

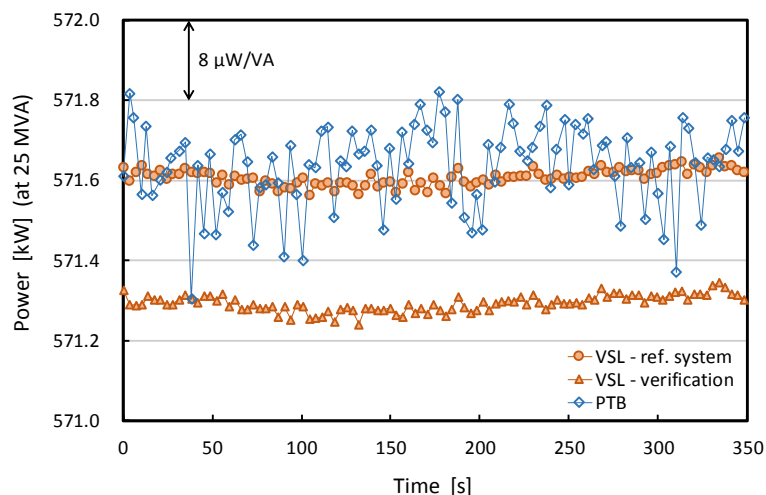


Figure 40 PTB – VSL system comparison 50 kV, 500 A, PF = 0.022, 51 Hz

#### 4.3.1.4 Conclusions

Two complementary approaches have been developed for the calibration of industrial TLM systems. The PTB approach uses parallel generation of voltage and current test signals, whereas the VSL approach generates the test current via a feedback loop that maintains a constant phase of the current with respect to the applied HV. Both setups are completely automated. The VSL setup furthermore is fully transportable and thus can be used on-site to calibrate TLM systems in the test halls of power transformer manufacturers.

A comparison of the PTB and VSL reference setups under laboratory conditions showed good agreement of both systems within 20  $\mu\text{W}/\text{VA}$ , and for currents less than 1000 A the agreement is even better than 12  $\mu\text{W}/\text{VA}$ . This result provides a very sound basis for the project's 50  $\mu\text{W}/\text{VA}$  target uncertainty claim for on-site calibrations at the premises of power transformer manufacturers.

### 4.3.2 Loss measurement on power capacitors and reactors

#### 4.3.2.1 Introduction

The determination of power capacitor loss and reactor loss is based on the use of capacitance bridges together with HV gas capacitors and CT. In case of reactor measurement this approach suffers from quadratic

dependence on the frequency, which makes balancing of the bridge difficult without additional compensation circuits.

However, sampling techniques combined with precise current and voltage sensors enable innovative methods for the precise measurement of both compensation capacitors and reactors. For example, a significant advantage of using Rogowski coils (RC) when measuring reactor losses is that their output voltage is the derivative of the current, which makes the loss current signal in phase with the voltage, and therefore the measurement becomes insensitive to frequency fluctuations. But by using modern high-resolution digitisers, comfortable and more flexible measuring systems can be built up without significant degradation of the accuracy compared to the current state of the art.

#### 4.3.2.2 Design of the Sampling Standards

##### *VTT sampling-based measuring system*

The principle of the VTT sampling-based measurement system is shown in Figure 41. The voltage  $\underline{U}_p$  across unknown impedance  $\underline{Z}$  is measured using a sampling multimeter. For voltages above 1000 V, a voltage divider can be used for precise voltage scaling. An RC is used to convert the current  $I_p$  flowing through  $\underline{Z}$  to a voltage, which is then measured by another sampling multimeter. The RC is shunted with a resistor  $R_T$  to compensate for the temperature dependence of the coil. On some measurements a current shunt was used instead of the RC to increase signal-to-noise ratio.

The two sampling multimeters receive their common trigger from a function generator. The sampling rate (approx. 4 kS/s) is adjusted so that typically 2048 samples are acquired during 25 periods. The complex impedance  $\underline{Z}$  can be calculated from the measured voltage ratio  $\underline{U}_p/\underline{U}_2$  with typical uncertainties below 10  $\mu\text{V}/\text{V}$  (or  $\mu\text{rad}$ ). The two-channel sampling system has also been used with e.g. for calibration of voltage and current transformers.

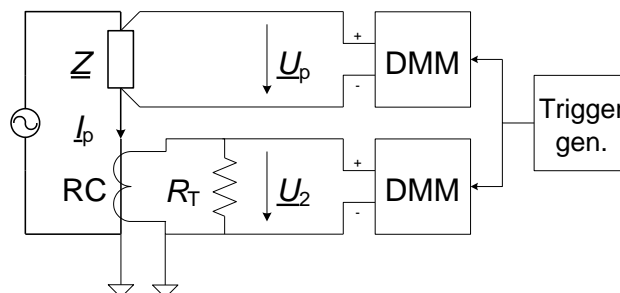


Figure 41. Principle of the VTT sampling-based measurement system.

##### *PTB sampling-based measuring system*

The principle of the sampling-based measuring system of PTB is shown in Figure 42. A set of calibrated VT and CT are connected to the impedance  $\underline{Z}$  in order to sense the HV  $\underline{U}_p$  and the high current  $I_p$ . The buffer at the low (Lo) terminal of  $\underline{Z}$  reduces the errors due to the loading effect by the voltage transformer. The voltage path consists of a cascade of a standard voltage transformer VT1 (error class 0.02) and a two-stage voltage transformer VT2 (error class 0.0005). The current path is built with an electronically compensated standard current transformer CT1 (error class 0.001) and a current comparator based current-to-voltage transformer CT2 (error class 0.0005). The low voltage outputs of VT2 and CT2 are connected to a precise two-channel sampling system. This system was originally developed for modernising instrument transformer measuring systems at PTB. It measures the complex voltage ratio of two voltages  $\underline{U}_2/\underline{U}_1$  with typical uncertainty in the order of 1  $\mu\text{V}/\text{V}$  (or  $\mu\text{rad}$ ). The digitiser is operated in an asynchronous sampling mode with a sampling rate of 50 kS/s. To minimise spectral leakage, an interpolation and resampling algorithm is used.

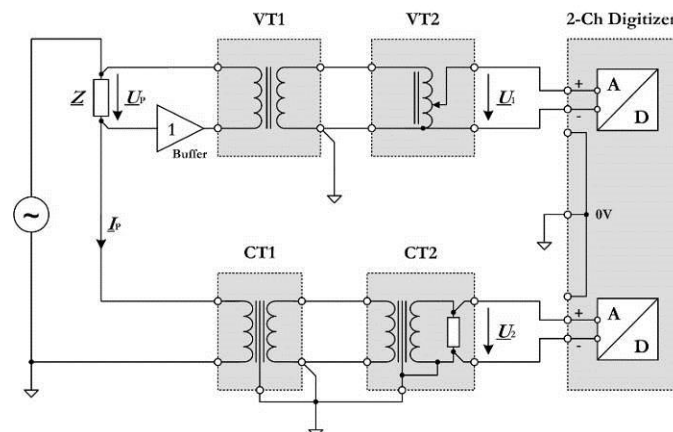


Figure 42 Principle of the PTB sampling-based measurement system.

#### Definitions for Loss Calculation

The losses of the impedance  $Z$  can be determined in different ways. The complex apparent power  $\underline{S} = P + jQ$  can be calculated from  $\underline{U} \cdot \underline{I}^*$ ,  $\underline{Z} \cdot I^2$  or  $\underline{Y} \cdot U^2$ , where  $\underline{I}^*$  and  $\underline{Y}$  stand for the conjugate complex current and the conjugate complex admittance of  $\underline{Z}^{-1}$ , respectively. The latter two definitions can be used in a ratio-based measurement system, when the rated conditions in terms of voltage or current cannot be attained during impedance measurement. In this case lower type A and type B uncertainties are attainable, as ratio measurements are usually more accurate than power measurements. The rated losses  $P_r$  are calculated from  $\text{Re}\{\underline{Z}\} \cdot I^2$  for the series reactor or  $\text{Re}\{\underline{Y}\} \cdot U^2$  for the shunt reactor or capacitor, respectively.

#### Measurements

The VTT and PTB measuring systems were compared by means of measuring on the same object. One comparison setup emulated the voltage and the current of a capacitor or a reactor using a phantom power source, driven by an active circuit with an integrator, differentiator and an adjustable loss part. Such a power source is useful for calibrating commercial HV loss power measuring systems, as every load can be emulated without providing the high reactive power usually needed.

Another setup for comparing the systems used a set of reactive components; a medium voltage air core reactor of 10 kVA, an adjustable low voltage shunt reactor with 15 kVA maximum, and a low voltage 20- $\mu\text{F}$  compensation capacitor. Using this setup, several tests at power line frequency were performed with varying test voltages or test currents. Agreement was better than  $100 \times 10^{-6}$  for iron core inductor loss measurements, and better than  $20 \times 10^{-6}$  for capacitance loss measurement. The measurement of the losses of air core inductor agreed within  $200 \times 10^{-6}$ , in this case the discrepancies of the results were caused by the self-heating of the DUT.

The VTT measuring system was used for calibration of a 25 H HV iron core reactor at power frequency. The calibration was performed on-site in a customer's HV test field. A HV capacitive divider with known phase error together with a current shunt were used for scaling of the signals. The measured inductance and loss tangent as function of applied voltage are shown in Figure 43. The estimated overall uncertainties of this on-site measurement were 100  $\mu\text{H}/\text{H}$  for inductance and  $100 \times 10^{-6}$  for loss tangent.

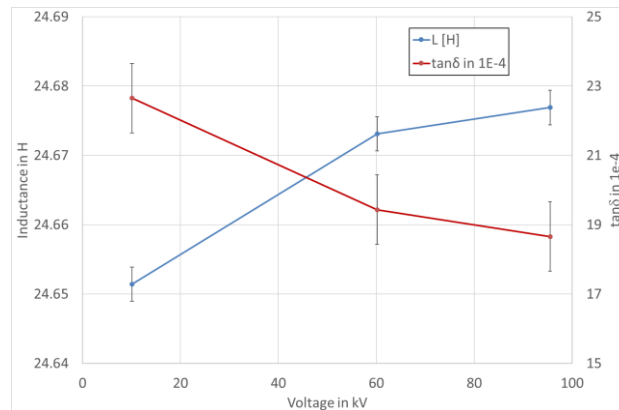


Figure 43 Result of on-site calibration of a HV iron core reactor at power frequency.

The VTT sampling-based measuring system was also used for calibration of high valued capacitors. A 53  $\mu\text{F}$  capacitor was calibrated both using a traditional current comparator bridge. The results of the comparison are shown in **Table 8**.

Table 8. Difference between current comparator and sampling system-based calibration a 53  $\mu\text{F}$  capacitor. Uncertainty of comparison was  $20 \mu\text{F}/\text{F}$  for capacitance and  $20 \cdot 10^{-6}$  for  $\tan \delta$ .

Voltage [V]	Capacitance in $\mu\text{F}/\text{F}$	$\tan \delta$ in $10^{-6}$
160	2	2
260	-7	4

#### 4.3.2.3 Conclusions

PTB and VTT have developed reference calibration systems for power reactors and capacitors with quite different technical approaches. Verification of their respective reference calibration systems was performed with reasonably good results. In addition, the VTT setup has been successfully used for on-site measurements. The challenging  $10 \mu\text{W}/\text{VA}$  uncertainty aimed for in the project was achieved under limited test conditions only. Future work is required to extend this uncertainty for a wider test range.

#### 4.3.3 Loss measurement on power cables

##### 4.3.3.1 Introduction

HV underground power cables are used to supply electrical power to large cities and cables with very large cross section conductors, up to  $2500 \text{ mm}^2$ , are used. Such large conductors are already at 50 Hz affected by the skin effect so that the AC resistance is larger than the DC resistance. It can be more than 50 % higher than the DC resistance, but the conductors can be designed to have lower AC resistance, e.g. by segmentation or using lacquered wires. Lower AC resistance is important as it will lower the loss in the electrical energy transport. Lower AC resistance is also needed as the maximum working temperature of the power cables,  $90^\circ\text{C}$ , sets a limit for the maximum current in the cable and hence the maximum transferred electrical power.

IEC 60287-1-1 is the standard method to determine the AC-resistance based on the DC resistance and on certain design parameters for cross section areas up to  $1600 \text{ mm}^2$ . CIGRÉ has found that the standard method is imperfect for the larger cross section areas in this range, which could lead to under-estimation of the loss and may be hazardous. Hence, CIGRÉ recommends the measurement of the AC resistance of such conductors when the cable is type tested, either by electrical or calorimetric methods. But, calorimetric methods are typically not as accurate as electrical methods.

However, very low loss power cables are made using lacquered wires in the conductor and it is not obvious that electrical methods are possible to use. Hence, a new calorimetric measuring method has been developed by the project, which aims to be as accurate as electrical methods are for segmented cables of standard design (approx.  $\pm 1 \%$ ).

4.3.3.2 Calorimetric measuring system

The basic principle of the new calorimetric measuring system is that two equal samples of a power cable are arranged in one AC and one DC current circuit, Figure 44. The AC and DC currents,  $I_{AC}$  and  $I_{DC}$ , are adjusted until the self-heating increase the temperature of the conductor of both samples to  $90^{\circ}\text{C}$  at the centres. The ratio of the AC resistance,  $R_{AC}$ , and the DC resistance,  $R_{DC}$ , of the conductor can then be determined as:

$$\frac{R_{AC}}{R_{DC}} = \frac{I_{DC}^2}{I_{AC}^2} \text{ when } \Delta T_2 = 0 \text{ and } T_{DC} = 90^{\circ}\text{C}$$

To assure that the temperature rises at the centres of the two samples are due to self-heating only, both ends of the two samples are cooled to the ambient temperature, approx.  $20^{\circ}\text{C}$ , see Figure 44, and kept at equal temperatures so that  $\Delta T_1 = \Delta T_3 = 0$ .

The use of two samples implies that the heat loss does not need to be measured, i.e. just made equal for both samples. So the cable samples need to be equally supported and have an uniform environment so that losses due to convection and radiation are the same for both samples.

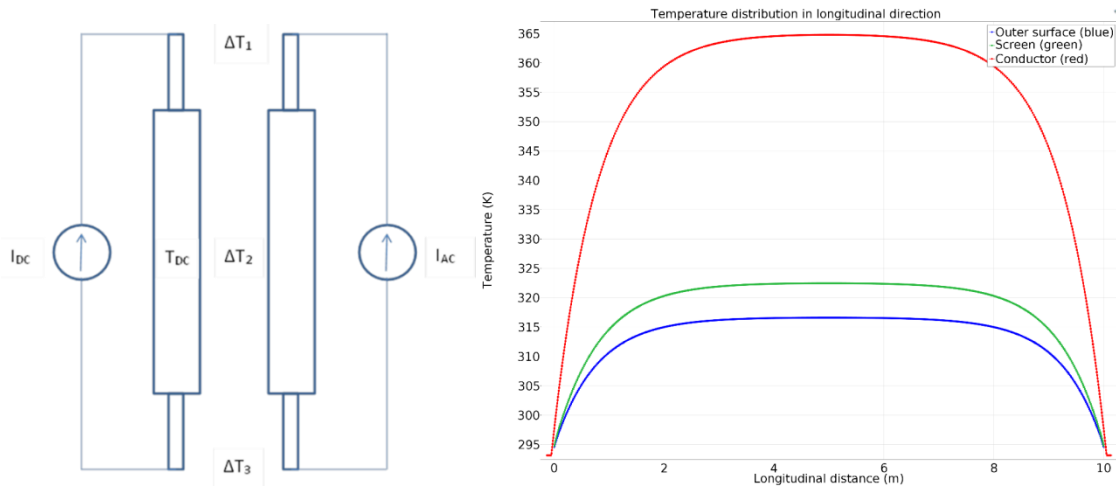


Figure 44. Schematic drawing showing the basic principle of the calorimetric measuring system with AC and DC circuits in parallel (left). Simulation of the temperature distribution along the cable conductor (red), screen (green) and outer surface (blue) in the AC circuit (right).

At the implementation of the calorimetric measuring system it was chosen to use one sample of a power cable and make consecutive measurements with AC and DC current, Figure 45. The main reason for this was the importance of the connection of the cable conductor to the current terminals. By using one sample the connection to the cable conductor was the same for both the AC and DC measurement. Other advantages were that the thermocouples, the emissivity and the support of the cable were the same at both measurements. Thus correlation of these sources of error could decrease the uncertainty and the mutual coupling between the AC and DC circuits is no longer an issue. However, this procedure also put more emphasis on controlling and measuring the ambient temperature and avoiding drafts as one doesn't have the advantage of an equal environment as when making parallel AC and DC measurements.



Figure 45. Measurement with AC current in the calorimetric measuring system.

#### 4.3.3.3 Electrical measuring system

The electrical measuring system used at RISE has been used several years to measure the AC and DC resistance of segmented cables of standard design. This type of cable is made of bare copper wires, however, to be able to measure very low loss power cables a different way of preparing the sample is needed that can be applied to cable conductor made of lacquered wires. Both ends of the cable conductor need to be opened, the lacquer removed and then closed again. The wires were then welded together in the ends to assure that the current connectors are in good contact with all wires. To allow the voltage terminals to be in contact with as many wires as possible along the circumference, the lacquer was removed for 10 mm by grinding. With this preparation it is possible to make measurements of the AC and DC resistance, but how accurate they are needed to be determined. For example, is the voltage potential of the outer layer of wires at a terminal a good representation of the potential of all the isolated wires in the cross section? A theoretical analysis by the project shows that it should be. But will the connection of the outer layer of wires caused by the voltage terminal influence the accuracy? The project hope to answer this question by a comparison between the electrical and calorimetric measuring systems.

#### 4.3.3.4 Comparison of the Electrical and Calorimetric measuring systems

The aim was to verify the accuracy of the measured ratio between the AC resistance and the DC resistance,  $R_{AC}/R_{DC}$ , of cables of a very low loss design. This was made in two steps: first by measuring on a cable of standard design and comparing the result of the calorimetric measuring systems with the result of the electrical measuring system, whose accuracy has been verified by calculable standards. Secondly by measuring on a cable of very low loss design and comparing the result of the electrical measuring systems with the result of calorimetric measuring systems, which operates without voltage terminals.

In both cases the measured values of  $R_{AC}/R_{DC}$  differ by approx. -4 % which looks consistent, see Table 9, but unfortunately the repeatability of the calorimetric measuring system causes an uncertainty of the same order. Additionally, the current terminals used in the calorimetric measuring system didn't allow welding of the cable ends and it was observed in the electrical measuring system that poor contact of the wires in the current terminals can cause a lower value of the measured ratio. Hence, it is unfortunately not possible to draw any conclusions on the accuracy based on these results. But what is obvious is that the connection of current terminals needs to be solved to make good measurements of the loss in cables of very low loss design.

**Table 9. Measured ratios  $R_{AC}/R_{DC}$  at 90°C**

	Calorimetric meas. system $R_{AC}/R_{DC}$	Electrical meas. system $R_{AC}/R_{DC}$	Difference in %
Cable, standard design	1,302	1,358	-4,1
Cable, very low loss design	1,019	1,056	-3,5

#### 4.3.3.5 Calorimetric measuring systems, three-phase measurement

An investigation of the influence on the loss in a cable conductor, of standard design, caused by the other two phases in a three-phase system was made. One cable was placed on each side of the cable in the calorimeter, Figure 45 at approx. 0.3 m distance, centre-centre. The AC current needed (approx. 3 kA) in the measured phase to get 90°C was measured with and without the same current (3 kA) in the surrounding phases. With this configuration the loss in the measured phase increased by 1.6 %  $\pm$  0.5 % due to the current in the two other phases.

#### 4.3.3.6 Conclusions

A calorimetric measuring system for measuring the ratio between AC and DC resistance of the conductor of HV power cables was developed and used to measure the ratio of the AC resistance relative the DC resistance,  $R_{AC}/R_{DC}$ , of a cable of low loss design. An uncertainty analysis predicted that the ratio  $R_{AC}/R_{DC}$  at 90° C of a 2500 mm<sup>2</sup> cable of low-loss design can be measured with an uncertainty of 1.0 %.

The ratio between AC and DC resistance of a cable of low loss design was measured by both electrical and calorimetric measuring systems. The value of the ratio  $R_{AC}/R_{DC}$  at 90° C measured by the calorimetric measuring systems is 5.0 % lower than the value measured by the electrical measuring system. Unfortunately, the uncertainty of the calorimetric measuring system, 7 %, is much larger than predicted so no conclusion can be drawn.

The influence of the temperature of the cable ends relative the ambient temperature and its uncertainty contribution needs to be further investigated. The importance of the connection of all wires in the current connectors is further emphasised, not only for measuring the loss in power cables of low loss design but also for making this type of cable a commercial product.

#### 4.4 Objective 4, HVDC convertor station loss

##### 4.4.1 Rationale

Losses of HVDC converter stations need to be accurately quantified to support evaluation of bids for such systems and to underpin efforts to reduce greenhouse gas emissions. Prior to the start of this project, these losses were estimated, based on loss calculations for individual converter components, and no reliable method existed to measure the actual HVDC converter station loss as a difference between power on the AC- and DC-side of the station.

In a previous EMRP project, ENG07 HVDC, a method was published for the determination of losses of an entire HVDC substation based on the connection of two converters in the same converter station, in a back-to-back configuration and circulating power between the two converters, whilst feeding from the AC power grid. An extension of this method was developed, where HVDC substation losses are determined using the difference between power measured on AC and DC sides respectively. The permissible uncertainty in respective measurements is very low and represents state-of-art and cannot be met by normal grid grade instruments and transducers. The requirements on the components of measuring systems thus need to be carefully analysed in terms of performance.

The necessary requirements for such a measurement were investigated in this project, and a tentative design of a suitable loss measuring setup was explored. This approach is a useful alternative for those cases where a direct measurement of losses via a temporary connection with two converters operating in back-to-back mode cannot be made.

##### 4.4.2 Measurement of HVDC station power

###### 4.4.2.1 Approach

The losses of a complete HVDC converter station can in principle be measured as the difference between input and output power as measured on its connections to the AC and DC transmission lines.

The envisioned setup is to use dedicated power measurement systems with state-of-art HV sensors and associated instruments. One such measuring system is a three-phase power measurement system connected to the AC grid and the other is single-pole power measurement system connected to the DC grid. In the case of the DC grid, an added complication is that DC transmissions are not normally connected directly to earth, but instead to a neutral bus running typically at some 5 % of the line voltage, and thus this necessitates measurement of voltage between line and neutral bus.

The basic formula for the direct measurement of HVDC converter station loss power  $P_{loss}$  is

$$P_{loss} = |P_{AC} - P_{DC}| \quad P_{loss} = |P_{AC} - P_{DC}| \quad P_{loss} = |P_{AC} - P_{DC}|, \quad (1)$$

with  $P_{AC}$  and  $P_{DC}$  the HV AC and DC power respectively, transmitted by the converter station.

To achieve an overall target of 3 % expanded uncertainty for an estimated converter loss of 1 %, the gross power must be measured with 0.03 % relative expanded uncertainty. A reasonable assumption is that the AC-side and DC-side power measurements  $P_{AC}$  and  $P_{DC}$  contribute equally to the final uncertainty, and that a third equally large contribution stems from unavoidable variation in readings during the measurements, therefore an uncertainty of at most  $0.03/\sqrt{3} \approx 0.017$  % should be achieved for each of the three uncertainty contributions. However, grid equipment in use in convertor stations is generally not intended for metering purposes and even the best guaranteed accuracy class of 0.1 % of metering equipment by far is not sufficient for the determination of converter station loss.

###### 4.4.2.2 AC power measurement

The accurate measurement of AC power  $P_{AC}$  follows the standard practice used in grid metering setups: the HV and current are scaled using precise VT and CT, and their outputs are measured with a precise power meter. So, for each phase, the AC power is determined via:

$$P_{AC} = \frac{1}{T} \int_0^T V_{HV}(t) \cdot I_{HV}(t) dt \approx V_{HV,rms} \cdot I_{HV,rms} \cdot \cos \varphi, \quad (2)$$

with  $V_{HV,rms}$  and  $I_{HV,rms}$  the root-mean-square (rms) values of the HV and high current respectively, and  $\varphi$  the phase between these two signals. Equation (2) assumes (for ease of discussion) sinusoidal voltage and current signals; the effect of inevitably present distortion is discussed in sub-section 4.4.2.4.

If we introduce the nominal VT and CT scaling factors  $k_{VN}$  and  $k_{CN}$  respectively, equation (2) becomes:

$$P_{AC} = k_{VN} \cdot k_{CN} \cdot P_W, \quad (3)$$

with  $P_W = V_{LV,rms} \cdot I_{LV,rms} \cdot \cos(\varphi)$  the AC power measured by the reference power meter connected to the outputs of the instrument transformers. As can be inferred from the formula for  $P_W$ , phase displacement will become important when the power factor is low. This will be the case when measuring no-load loss.

When developing the uncertainty budget for this measurement, it can be seen that the contributions listed in Table 10 dominate.

**Table 10 – Estimation of necessary uncertainties in AC power measuring system**

Quantity	Expanded relative uncertainty	Value
CT ratio error	$U_C$	0.015 %
VT ratio error	$U_V$	0.015 %
Power meter	$U_{PW}$	0.015 %
Phase displacement	$U_{FD}$	0.09 mrad

The requirements listed are far more stringent than the best standard equipment for grid use can fulfil. One of the partners (VSL) has however developed HV CT and VT that have been verified to perform even better than required, and uncertainties of approximately 1/3 of those in Table 10 have been achieved. A similar situation is currently under development for the power meter, with an expected uncertainty in the range 0.01 to 0.005 %.

Combining the uncertainties of the CTs, VTs, and reference power meter, an overall uncertainty in the AC power measurement of better than 0.01 % is achieved, well below the target of 0.017 %.

#### 4.4.2.3 DC power measurement

Power measurement on the DC side of HVDC converter stations follows the same basic approach as on the AC side. It requires accurate DC current transducers and DC voltage dividers. DC power metering can in principle be performed with dedicated DC responsive power meters, but in the case of verification measurements, the use of high-precision multimeters combined with suitable software forms a very good alternative.

Measurement of the HVDC station DC voltage output poses a challenge since the low voltage terminal is normally not at earth potential. Several connection schemes are used, e.g. having an earth electrode at some distance from the converter station or using two converters in a bi-pole connection where a common point is at low potential, or the case of metallic return where the low voltage terminal is routed via cable or overhead line to the other end of the intertie. These examples unequivocally show that it is necessary to measure the voltage between the low voltage and HV terminals of the HVDC station. Connecting the voltage divider between these terminals would be preferable from the point of reducing uncertainty, but the problems of arranging the insulation of the instrumentation connected to the low voltage output prohibit a solution. Thus a separate voltage divider for measurement of the neutral bus voltage must be considered. The normal operating voltage of a neutral bus is often in the range of less than 5 % of the line voltage, so that even solutions with moderate accuracy can be considered. The insulation level, should however be such that the voltage divider can withstand the voltage that can occur during faults. These voltages will be specific for each installation and determined in system studies. However, a general estimate is that short-time stress (e.g. events similar to switching impulse) can be on the order of 25 % of the line voltage.

The result of a measuring system for DC power can be written as:

$$P_{DC} = SF_C \cdot V_C \cdot (SF_V \cdot V_V - SF_{VN} \cdot V_{VN}) \quad (4)$$

where

- $P_{DC}$  Power measured on DC side with a combined absolute standard uncertainty  $\hat{u}_c^2(P_{DC})$
- $SF_C$  Actual scale factor of the DC current transducer in V/A, calibrated with a relative standard uncertainty  $u_{SF_C}$
- $V_C$  Output voltage of the DC current transducer in V, measured with a relative standard uncertainty  $u_{V_C}$
- $SF_V$  Actual scale factor of the DC line voltage divider in V/V, calibrated with a relative standard uncertainty  $u_{SF_V}$
- $V_V$  Output voltage of the DC line voltage divider in V, measured with a relative standard uncertainty  $u_{V_V}$
- $SF_{VN}$  Actual scale factor of the DC neutral bus voltage divider in V/V, calibrated with a relative standard uncertainty  $u_{SF_{VN}}$
- $V_{VN}$  Output voltage of the DC neutral bus voltage divider in V, measured with a relative standard uncertainty  $u_{V_{VN}}$

Since equation (4) consists of both products and sums, formal development of an uncertainty budget becomes complex, but can be considerably simplified if one considers that neutral bus voltage is much lower than line voltage.

In sub-section 4.4.2.1 above, a suggested performance requirement for the DC-side power measurement was given as 0.017 % relative expanded uncertainty. In the first analysis, uncertainties of measuring instruments can be neglected since precision DC voltmeters with uncertainties down to a few parts per million are readily available.

Assuming that the uncertainty is of the same magnitude for both voltage and current sensors, we arrive at an estimate of 0.012 % for the expanded uncertainty, which can be broken down into estimates as given in Table 11.

**Table 11 – Estimation of necessary uncertainties in DC power measuring systems**

Quantity	Component	Contribution to relative standard uncertainty	Value [%]
Current transducer, scale factor	$SF_C$	$u_{SF_C}$	0.01
Instrument for voltage of current transducer	$V_C$	$u_{V_C}$	Negligible
Line voltage divider, scale factor	$SF_V$	$1.21 \cdot u_{SF_V}$	0.01 %
Instrument for line voltage of voltage divider	$V_V$	$1.21 \cdot u_{V_V}$	negligible
Neutral bus voltage divider, scale factor	$SF_{VN}$	$0.12 \cdot u_{SF_{VN}}$	0.05
Instrument for neutral bus voltage of voltage divider	$V_{VN}$	$0.12 \cdot u_{V_{VN}}$	negligible

DC current sensors for high-precision application at high current are often realised using DC current transducers using zero-flux technology. This technology has been developed in the 1960s as well as for use in HVDC converter stations in the late 1970s. The performance of these devices has been shown to be on the order of a few parts in  $10^5$  and is thus eminently suited. Calibration facilities for these devices are available at several NMIs world-wide including RISE.

However, a significant challenge is the HV insulation required if the measurement is to be performed on the HV bus. Fortunately, this can be circumvented by realising that the neutral bus will carry the same current, reducing insulation requirements drastically. In fact, there is a possibility to use a low voltage measuring head with a piece of HV cable routed through the opening of the toroidal measuring head. The estimated best performance for the DC current sensor is 0.004 %.

DC voltage dividers can be made for voltages up to more than 1000 kV and for use in HVDC stations. Provided they are stable enough, a calibration can be performed to verify the stability. A development in previous project EMRP ENG07, has made available 1000 kV reference dividers with a best uncertainty of 0.002 %. One of these dividers is of modular design and can be used directly in an on-site measurement of voltage on an HVDC station busbar. The estimated best performance for the DC line voltage divider is 0.004 %. Performance of state-of-art voltmeters can be estimated as 0.001 %.

Combining the uncertainties of the current and voltage sensors and of the voltmeters, an overall uncertainty in the DC power measurement of better than 0.006 % is achieved, well below the target of 0.017 %.

#### 4.4.2.4 *Influencing factors*

The effect of harmonic distortion on the AC side can be viewed in several different approximations. For example, one approximation is that there may be harmonic distortion on the supply voltage on the electrical grid, which should be taken into account. Or conversely, a converter station can generate harmonic distortion due to the operation of the HVDC valves. In first approximation, the converter can be viewed as current source for harmonic currents. These currents lead to a corresponding harmonic voltage that depends on the impedance of the connected grid. What is important here, is that the harmonic power is fed into the grid. To clarify, this means that the harmonic power is added to the power drawn from the grid, either increasing or decreasing the apparent value of the AC power. A suggestion to counter this is to only consider the power at the fundamental frequency, but this choice is by no means uncontroversial, and further discussion is required. If the harmonic power is included in the evaluation, the AC power meter should be verified on the accuracy of its harmonic power measurement capabilities. For modern, sampling-based power meters this should not be a significant problem, especially since any harmonic power will only be a fraction of the fundamental power.

On the DC side, any effect of harmonic power will be removed by the integration over time of measured quantities and can thus be disregarded.

The intention of the loss determination is to quantify the converter station loss. Therefore, all primary transducers (AC voltage and CT, DC dividers and current transducers) should be close to the station inputs and outputs in order to be sure to include all filters etc. in the loss determination.

A significant benefit from this is that the action of filters will relieve some of the concerns for effect of harmonics on the AC-side power measurement, due to the mitigation by the filters.

The HVDC converter station forms a harsh electromagnetic (EM) environment for the precision power measurements, which easily and negatively affects the measurement accuracy. Therefore, extensive attention has to be paid to correct shielding and grounding of the AC- and DC-power measurement setups. Effective shielding can be achieved in such on-site conditions via the use of double-shielded twisted pair cables connecting the instrument transformers with the power meters. The outer shield of these cables is connected to ground at both ends of the cable and used as a safety ground. The inner shield serves as a measurement ground and only is connected at one side of the cable, typically at the side of the instrument transformer.

For the grounding, a central ground should be used as much as possible, and ground loops should be prevented in the measurement circuit. For the DC-side power measurement, special care has to be taken to minimise DC offsets in the voltage measurement circuits.

The possible occurrence of both EM interference and ground loops can be significantly reduced by minimising the length of the secondary wiring between the instrument transformers and the power meters, and placement of the AC- and DC-power measurement equipment in shielded racks. Readout of these shielded racks can subsequently be arranged with fibre readout.

#### 4.4.2.5 *Conclusions*

The feasibility for direct determination of HVDC converter station loss by measuring the difference of station output power and input power was explored. For achieving an overall 3 % uncertainty in a typical 1 % station loss power, the AC- and DC-side power measurements each have to achieve better than approx. 0.017 % uncertainty. Careful evaluation of the respective AC- and DC-power uncertainty budgets show that such uncertainties indeed appear achievable using state-of-the-art measurement instrumentation. Particular details of the DC-power measurement are the voltage measurement of both the HV and low-voltage busbar, and the current measurement in the low-voltage busbar.

Spurious effects, possibly affecting the overall loss measurement accuracy were carefully evaluated. These include operating conditions, harmonic distortion, measurement position, EM interference, and instrument transformer burden. Several recommendations were drawn from this evaluation, such as the use of short, double-shielded secondary cables and calibration of the instrument transformers with the burden using in the actual HVDC station loss measurement.

In summary, this study has shown that direct measurement of HVDC converter station losses, as the difference measurement of AC- and DC-power, is indeed achievable with 3 % uncertainty for HVDC converter station loss power levels of 1 %. This is a significant step forward with respect to the present state of the art for

measurement of converter loss, reflected in the two main IEC standards i.e. IEC 61803 and IEC 62751-1 related to HVDC converter losses, where HVDC converter station losses are estimated by summing the losses calculated for each item of equipment. The project's proposed approach achieves much better uncertainty and moreover does not rely either on assumptions concerning converter station component behaviour or on the (inherently imperfect) characterisation of these components. Ideally, the proposed direct loss measurement should be applied on the entire converter station as a routine measure after delivery, or at least as a validation of the calculation and estimation methods used.

#### 4.4.3 Non-invasive current transformer: Prototype compact, distributed digitiser

During this project a prototype compact, distributed digitiser was developed for the readout of a non-invasive reference current sensor that was initially developed in the preceding project EMRP ENG07. This digitiser also enables complex measurements by combining several measurement nodes into a network. The digitising nodes have state-of-the-art timing synchronisation and amplitude resolution that comply with the requirements of the most demanding metrology applications. The use of fibre readout and time synchronisation allow applications for the distributed digitiser with special isolation requirements, such as in the HV area, as well as extending the distance over which they can be used to several hundreds of meters. Envisaged applications of these distributed digitisers include the high-accuracy measurement of currents and voltages in substations of the electricity grid, power quality propagation in low-voltage networks, and calibration of non-conventional VT and CT with digital outputs (using e.g. the IEC61850-9 protocol).

To make the distributed digitisers versatile and suitable for a variety of applications, they need to have audio frequency bandwidth and be able to report raw samples with sufficiently high resolution. This makes the communication bandwidth high, ruling out wireless read-out options. Furthermore, GPS is not accurate enough for time synchronisation and would limit the use of the distributed digitiser to outdoor use only.

Due to this, white rabbit (WR) technology was chosen since this offers both accurate timing and high bandwidth communication. The design of the system is shown in *Figure 46*. Within each digitising node, the WR-engine takes care of synchronisation and communication with the central WR-switch via optic fibre. A central processing unit (CPU) board with several Mbytes of memory and infrastructure for a Transmission Control Protocol/Internet Protocol (TCP/IP) stack is used for running a high-level programming environment. The micro controller unit (MCU) acts as interface and buffer between the ADC and CPU. The ADC evaluation board contains the analog front-end and the voltage reference. A high-resolution 24-bit Delta-Sigma ADC with an oversampling ratio of 512 is used, resulting in an effective sampling speed of 19531.25 sample / s (10 MHz / 512). The master controller is used to aggregate all samples and perform the final calculations. The master WR-node which is the time reference for all units is in the network and can be synchronised with a master clock or UTC realisation.

Data readout of the ADC is via adding a bare-metal MCU between the ADC and the CPU. This MCU's only task is to read out the ADC. The data is collected by the MCU, buffered and sent in bigger blocks to the Linux system, which then handles the ethernet task.

Data acquisition is started by sending an arming signal to all digitising nodes. Then a trigger is set on each unit to occur at a specified point in time. Since all nodes are "perfectly" synchronised to the master, all ADCs and counters are synchronised and will be triggered at the same instant in time. The nodes subsequently collect the desired number of samples and send them over to the master controller for further data processing.

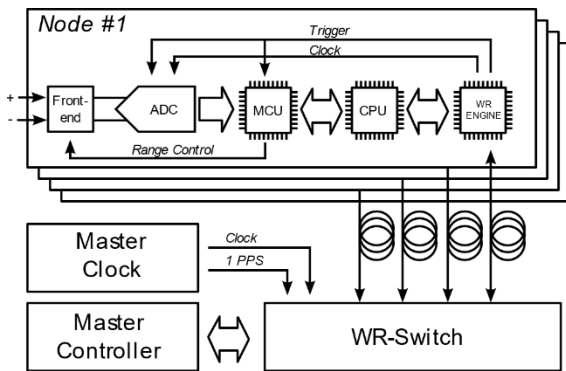


Figure 46: System block diagram showing several digitising nodes connected to a central switch, and a master controller to aggregate the raw samples of all nodes. The master clock synchronises the nodes via WR technology. Each node consists of a WR-Engine, a CPU, and a MCU as interface between the ADC and CPU..

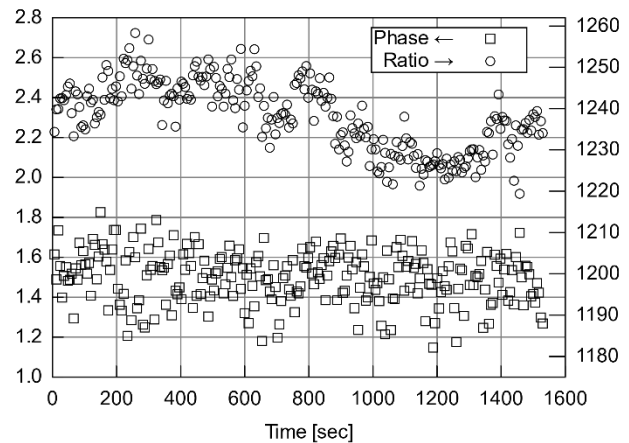


Figure 47: Phase difference and ratio error between two digitising nodes, both measuring the same 60 Hz sine wave with an amplitude of 2 Vpp.

Measurements were performed to assess the performance and stability of the system in both magnitude and phase. Figure 47 shows the result of a 25 minute measurement where a 60 Hz sine wave with 2 Vpp amplitude has been applied to two digitising nodes. The measured phase difference of  $1.5 \pm 0.1 \mu\text{rad}$ , corresponding to approx. 4 ns time delay, can be partly explained by the 1 ns delay that was observed between both trigger signals. This delay can be further reduced by calibrating the small form-factor pluggable transceiver modules and optical fibre to the sub-nanosecond level. The remaining ~approx. 3 ns delay likely is caused by the limited slew rate of the triggering signals. The short-term amplitude performance is good but the long-term stability is severely limited by the temperature dependence of both the gain of the ADC and the reference voltage. In Figure 47, the ratio of the measured magnitudes is  $1240 \pm 5 \text{ ppm}$ . This 0.1 % difference can be corrected for by implementing gain constants in the different digitiser nodes. However, what remains after the correction is the long-term stability of the ADC front-end including voltage reference gain, as well as their temperature dependencies. With the present choice of ADC and voltage reference, the latter is around  $30 \mu\text{V/V}/^\circ\text{K}$ , which is clearly insufficient for the intended applications.

After some major software improvements, a second set of measurements were performed where VSL compared their CT calibration setup with the developed distributed digitiser, by calibration with the openable core current transformer (OCCT) developed by VSL in previous project ENG07. Figure 48 shows the measurement setup where multiple frequencies from 45 – 65 Hz with 1000 A current were applied to the CTs measured via a shunt with the two digitisers. The phase measured difference of  $3 \pm 0.4 \mu\text{rad}$ , corresponds with about 9 ns time delay. The amplitude measurement is the same as the previous measurements.

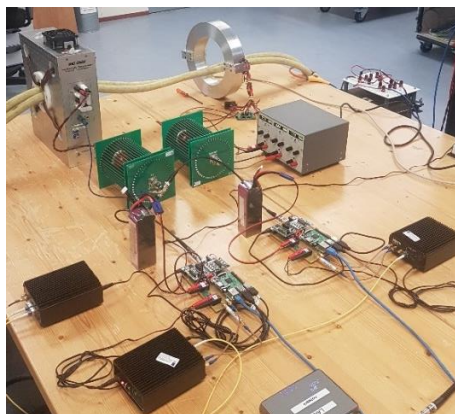


Figure 48: Measurement comparison the developed digitiser against the VSL CT calibration setup with the VSL developed OCCT

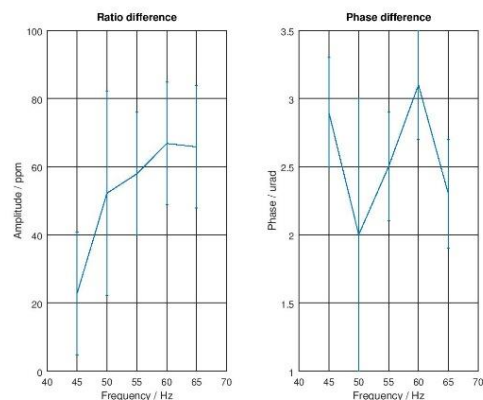


Figure 49: Results from the OCCT calibration

Even though the present system meets the project aims, several further improvements can still be made to the system. The gain-stability of the ADC and voltage reference can be improved, by using a temperature-stabilised voltage reference. The overall power consumption of the system can also be reduced, so that longer-period measurements can be done under battery operation. The maximum power consumption of the present system is approximately 7.5 W and this high consumption rules out powering the digitising nodes over optical fibre. When the use of mains power is not possible, the nodes will be battery powered to allow for as many applications as possible and to ensure a reasonably long measurement time.

In conclusion, a prototype compact, distributed digitiser has been developed for isolated readout of a non-invasive current sensor. The synchronisation, high resolution and fibre isolation makes this digitiser a versatile tool for on-site measurements. Initial results show that the device is very accurate in phase but it still needs improvements in amplitude. Improvements for future nodes can be implemented in future projects.

## 4.5 Results summary

### 4.5.1 Ultra-high impulse voltage testing

- New reference dividers for LI have been developed and characterised (PTB 1000 kV, RISE 500 and 800 kV)
- For the first time ever, intercomparison of measuring systems for LI has been performed (PTB, RISE and VTT) at an accuracy level better than any preceding comparisons.
- CMCs will be revised as a result of the project, with lower uncertainties for the measurands (voltage and time parameters) and for higher test voltages.
- The step response of a selection of transient recorders has been analysed, with the results indicating that very few available devices can provide accurate enough information. The work has led to methods to unequivocally separate devices with acceptable performance from those with unacceptable performance.
- Step voltage generators have been developed and characterised for the purpose of qualifying transient recorders. Their performance has been shown to include a rise-time down to less than 0.5 ns and a reliable settling to final value within 0.5 % after a few ns.
- It has been shown that convolution methods can be used to predict errors of a measurement device, e.g. a transient recorder or a voltage divider. Briefly the convolution methods include: an assumed input waveshape is convolved with the step response of the device, and the resulting output waveform is compared to the input, with the difference understood as error.
- Deconvolution methods have been developed and applied for correction of measured waveforms. In this deconvolution method, the input waveshape is deduced from inverse convolution of the output waveshape with the step response of the device.
- Step response has been investigated for several UHV class LI dividers in order to characterise the impact of the geometry of large measurement circuits. This has shown that the size of the loop from the test object to LI divider has a profound effect on the response, whereas the proximity to walls has appreciably less effect. This is not clearly reflected in the current relevant documentary standards and will be brought to the attention of the appropriate IEC committee.
- Calibration methods have been applied to several UHV class dividers and it has been shown that reliable calibrations for amplitude can be achieved at an uncertainty of 0.5 %. The uncertainty for front time suffers from problems in achieving LI without oscillations on the front.
- Investigations of difference in front time error as predicted by step response and convolution versus results obtained in HV calibrations have revealed that the difference in response in the reference divider (fast and showing oscillations) and the UHV divider (slow and acting more or less as a first order filter) is quite marked in the rising portion of the front. This phenomenon is not fully understood and should be further investigated. It will be brought to the attention of the appropriate IEC committee.
- Methods for extension of linearity of UHV measuring systems from 800 kV up to 3500 kV have been evaluated. The results is that only comparison of peak voltage with charging voltage can be recommended.
- The project has increased the maximum voltage levels for traceable LI calibration and has identified methods to reliably prove linearity up to UHV levels.

### 4.5.2 Very fast transients

- A state-of-art divider for VFT at 500 kV and 200 ns rise-time, has been developed and characterised.
- New CMCs for VFT will be submitted by RISE and VTT based on the research.
- Suitable test setup for insulator puncture tests with VFT has been identified.
- Early uptake has been achieved in the sales of the divider developed both to puncture test labs and to research organisations
- A master's thesis has been achieved as part of the research on measurement of VFT.
- Recommendations for puncture testing based on the results of the research have been presented to pre-normative group D1.60 within CIGRÉ.
- Methods for step response of sensors for current have been developed by partners VTT, Aalto and PTB, and their interaction has been important for the outcome.

- Generation of step current up to 100 A and with rise-time of a few ns has been accomplished. The length of the step is limited by the length of the cable used as generator, but an impressive 1  $\mu$ s length has been achieved.
- A second master's thesis has been achieved as part of the research on generation and measurement of fast current transients.
- New capabilities, hitherto not available, have been created for characterisation of fast current sensors and new CMCs will be submitted by VTT and PTB.

#### 4.5.3 Losses of power transformers, reactors and capacitors

- An in-house circuit for generation of phantom loss power developed by PTB uses parallel generation of voltage and current test signals.
- An on-site circuit for generation of phantom loss power developed by VSL generates the test current via a feedback loop that maintains a constant phase of the current with respect to the applied HV. This setup can also be used on-site to calibrate TLM systems in the test halls of power transformer manufacturers.
- A comparison of the PTB and VSL reference setups under laboratory conditions showed agreement of both systems within 20  $\mu$ W/VA, and for currents less than 1000 A. The agreement is even better than 12  $\mu$ W/VA. This result provides a very sound basis for the 50  $\mu$ W/VA project uncertainty claim for on-site calibrations at the premises of power transformer manufacturers.
- New CMCs have been announced by PTB and VSL for calibration of transformer loss measuring systems at an uncertainty level not reached before
- Sampling type measuring systems intended for loss measurement on power capacitors and air core reactors have been independently developed by partners VTT and PTB, using different approaches. An intercomparison has proven good agreement between the systems
- The challenging 10  $\mu$ W/VA uncertainty aimed for in the project was achieved under limited test conditions. However, further work is required to extend this uncertainty for a wider test range.
- A calorimetric system for losses on large power cables has been developed, based on measuring AC and DC current magnitude necessary to reach a specific conductor temperature.
- The calorimetric system has the advantage of being able to be applied to extreme low loss cables with insulated strands where existing electrical methods are difficult to apply.
- Tests performed uncovered several experimental challenges such as achieving stable and low temperature at the ends of the cable and maintaining stable current in the face of varying mains supply voltage that precluded reaching the desired uncertainty for the calorimetric method, which needs further research. However, development is important for the field and will be presented to industrial stakeholders at the Jicable 2019 - International Conference on cables and LV, MV, HV & EHV cables and cable systems.

#### 4.5.4 HVDC convertor station loss

- A methodology for the determination of loss a complete converter station has been developed. The method's feasibility has been investigated and suitable equipment has been identified for use with it
- A paper has been drafted that shows that 3 % relative uncertainty on a 1 % loss level is achievable with the method
- Contact has been established with CIGRÉ B4 to suggest that the output of this research be used in pre-normative work for determination of loss in converters.
- Based on development in a preceding EMRP project ENG07 HVDC, a non-invasive current transformer reference has been further developed to enable remote reading.

#### 4.5.5 Collaboration

Collaborative efforts have been instrumental in achieving the success of the project, especially in

- Ultra-high LI measurements where complementary skills and experiences were successfully used between PTB and RISE and supported by ABB (formerly STRI).
- The success of the work in objective 1 has resulted from an excellent cooperation between the partners including several secondments. Hence the results would have been very difficult for any single partner to achieve on their own.

- VFT in current circuits, where explored using different solutions by different partners PTB and VSL , including good cooperation between two Phd. students
- Loss measuring systems for transformer loss, where the difficult problem of power measurement at power factor close to zero was tackled by VSL and PTB using different solutions and decisively aided by the work of a Post Doc at TU Delft
- Two senior researchers from RISE and VSL have combined forces to address the HVDC converter station loss challenge, using their complementary knowledge.

## 5 Impact

The output of the project has been disseminated via publications in international journals, presentations at scientific and industry conferences, the organisation of workshops, and by active participation in international standardisation committees. Together with active participation of the project stakeholder committee members, this has ensured that the project outputs were effectively disseminated to, and exploited by the electrical power industry. Furthermore, it has facilitated the early take-up of several of the technological and measurement infrastructures developed by the project.

### 5.1 Dissemination activities

#### 5.1.1 Scientific publications and trade journals

The project has generated 22 high-impact publications in key journals out of which seven are in preparation. These publications incorporate the significant scientific outputs of the project. In addition, the project has led to two accepted Master's Theses. A full list of all project publications is given in chapter 6.

A manuscript describing the project has been submitted to the Swedish trade journal "ENERGI" <http://www.e-magasin.se/paper/srj0csg0/paper/1#/paper/srj0csg0> "

#### 5.1.2 Effective cooperation between project partners

EMPIR is a metrology-focused European programme of coordinated R&D aimed at facilitating closer integration of national research programmes and ensuring collaboration between NMI, reducing duplication and increasing impact. This project has been a good example of the implementation of this programme, gathering 5 NMIs, 3 academic partners, and 2 industries from 5 European Countries.

Much of the work in the project was very collaborative and effective cooperation between the project partners was essential to its success. Three particular examples are:

- Work visit of VTT to PTB in order to compare the respective reference setups for loss measurement of HV shunt reactors and power capacitors.
- Work visit of VSL to PTB in order to compare the respective reference setups for loss measurement of HV power transformers.
- Two extensive joint measurement campaigns of RISE, VTT, PTB, and ABB, for testing and comparing reference setups for UHV LI measurements.

#### 5.1.3 Conferences and relevant fora

An important aspect of dissemination is the interaction with scientists, researchers and industry specialists. Three major events have been identified in this respect, the biannual events Conference on Precision Electromagnetic Measurements (CPEM), International Symposium on High-voltage Engineering (ISH) and International Conference on High Voltage Engineering and Application (ICHVE). Each of these have attendance of about 400 delegates with world-wide provenance. Additionally, we have targeted International Conference on Electricity Distribution (CIRED) and IEEE International Workshop on Applied Measurements for Power Systems (IEEE AMPS). At these events a total of 21 contributions from the project were presented. In particular the CIRED and ISH conferences had significant industry participation, and therefore provided ample room for interaction with stakeholders/end users on the project's outputs.

#### 5.1.4 Stakeholder engagement

There was significant stakeholder engagement in the project's outputs:

- In the research on improved facilities for UHV LI measurements there has been active interaction with HighVolt and AMOTronics, two European manufacturers of LI measurement equipment.
- In the process of selection of suitable transient recorder for LI measurements, RISE has given important feedback to the international manufacturer National Instruments, leading to deeper understanding by the manufacturer of the needs in respect of LI. As a result this cooperation has led to ameliorations in the design of a new transient recorder, which has now been deployed by RISE in another EMPIR project 15NRM02 UHV (Techniques for ultra-high voltage and very fast transients).
- The VTT reference system was validated on its suitability for actual on-site measurement of losses of HV reactors and capacitors in the HV test field of one of the project stakeholders.
- Royal Smit Transformers, the Netherlands, gave VSL access to their HV power transformer test laboratory. This allowed VSL to test its new reference setup for calibration of industrial power TLM

systems, under the actual on-site conditions of an industrial test laboratory. The results of this test provided important input for further improvement of the VSL reference setup in the final year of the project.

#### 5.1.5 Engagement with Standards Development Organisations

The project partners have been very active within several normative and pre-normative groups to disseminate the project findings:

- Pre-normative group CIGRE D1.60 Traceable measurement techniques for VFT, where direct feedback from the work on VFT has been made by partners VTT and RISE.
- Documentary standards group IEC TC20, Electrical cables has been kept informed on the progress in methods to measure losses of power cables, through partner NKT HV.
- A major contribution was given to CENELEC TC14 and IEC TC14 as part of the revision of documentary standard CENELEC 60076-19 and IEC 60076-19, "Power transformers - Part 19: Rules for the determination of uncertainties in the measurement of losses in power transformers and reactors". Both RISE and VSL provided their input to this documentary standard as experts in the maintenance team and RISE furthermore served as Convenor of the IEC 60076-19 maintenance team.
- Further contributions were given to CENELEC TC14, Power transformers, via presentations and project updates presented at their regular 6-month TC14 meetings. Since loss measurements are one of the most significant tests performed on new power transformers, the CENELEC TC14 members showed great interest in the project's efforts. This interest also resulted in a few on-site calibrations of industrial loss measurement systems, performed by VSL using the reference setup developed in the project.
- Next to the contributions to CENELEC TC14 and IEC TC14, RISE and VSL provided information on the project results in loss measurements of reactors, capacitors and power transformers to their colleague members in the national TC14 mirror committees in SEK and NEC respectively.
- RISE participated in the Swedish national mirror committee TK22F (to SC22F), Power electronics for electrical transmission and distribution systems, where information of outcome of the work on loss measurement of HVDC substations has been given.
- Participation in Swedish national mirror committee TK 115, HVDC transmission over 100 kV where information of outcome of the work on loss measurement of HVDC substations has been given.

#### 5.1.6 Ecodesign Directive and Market Surveillance

VSL actively participated in several workshops organised by the EU on the review of the requirements posed by the Ecodesign Directive on power transformer losses. The discussions particularly focussed on the enhanced 'tier 2' requirements that are supposed to become valid per 1 July 2021.

Input was also provided by VSL to a workshop organised by Market Surveillance Authorities (MSAs) that must verify that the Ecodesign Directive is correctly implemented. The challenge concerning the requirements on power transformers is that it is too complex to perform verification measurements on installed units. In the workshop, VSL provided suggestions for other metrologically sound ways of effective market surveillance on power transformers. RISE provided actual market surveillance support to the MSA in Sweden.

### 5.2 **Impact on industrial and other user communities**

The core of the project has been the support of the European HV power industry via the improvement, and extension of, the HV metrology infrastructure in fields of loss determination and HV testing. The following project outputs have already provided benefits to industrial end-users and stakeholders:

- Development of calibration and linearity extension for LI measurements for future UHV transmission (in response to needs expressed by IEC). End users benefit from better quality control of HV transmission system components, which leads to more cost-effective solutions for UHV power transmission. A major impact of the project is enhanced confidence in the reliability of LI tests at the UHV.
- Improved test setups for puncture test on HV line insulators. This supports the compatibility of testing between different test organisations and enables accurate measurements via development of calibration services. End users benefit from better quality control of HV transmission system components, leading to more cost-effective solutions. This impact has been proven via the purchase of the puncture test system developed in the project by two commercial laboratories ABB (formerly STRI), Sweden and Verescence La Granja, Spain, both involved in insulator testing..

- Reference measuring systems and calibration methods for very fast current transients have been made available to industry and provide support for future standards development.
- New, highly-accurate test facilities for loss measurements on HV air-core reactors and power capacitors. These facilities are important tools for manufacturers to verify the quality of their products. During the project on-site calibration of such products has been performed by VTT.
- Enhanced loss measurement capabilities to support procurement of new systems or components for electricity transport as required in the Ecodesign Directive. Target beneficiary groups are transmission system operators (TSO) and major equipment manufacturers. These stakeholders, as present in CENELEC TC14, indeed have shown significant interest in the new facilities developed in the project. On-site calibrations performed by VSL using the new facilities have already helped power transformer manufacturers in verifying the quality of their products.
- A metrological infrastructure for loss measurement on large power transformers and converter valves by providing proper calibration services. Beneficiaries are manufacturers and purchasers of such equipment.
- A calorimetric measuring system for measuring the ratio between AC and DC resistance of the conductor of HV power cables has been developed and used to measure the ratio of the AC resistance relative the DC resistance,  $R_{AC}/R_{DC}$ , of a cable of low loss design. An uncertainty analysis predicts that the ratio  $R_{AC}/R_{DC}$  at 90°C of a 2500 mm<sup>2</sup> cable of low-loss design can be measured with an uncertainty of 1.0 %.
- Long term non-intrusive calibrations and an in-situ determination of a non-linear response in CT in substations for 400 kV power grids by an improved non-invasive current sensor. This will be beneficial for TSOs and legislators.
- The enhanced capabilities created for measurement of ultra-high LI ensures that production margins for the tested equipment can be reliably established, leading to more economic designs where optimised usage of materials is supported. The outcome will be that resources for construction are optimally used, with lowered energy used in manufacturing.
- The enhanced capabilities in measurement of loss has a twofold impact, firstly it enables optimisation of e.g. transformers with respect to materials usage, and secondly it provides a quality assured verdict of the actual efficiency of the HV equipment, promoting the choice of low-loss equipment. Again, the outcome will be that resources are optimally used in construction, and that equipment with consistently lower losses can be deployed into the electrical transmission system.

### 5.3 Early uptake of project results

Early uptakes of the project results have been achieved by

- Project partner RISE with Energimyndigheten (the Swedish Energy Agency). RISE has evaluated an industrial loss measurement on a large transformer (100 kVA, 11 kV) to support Energimyndigheten's investigation of its conformance to the Ecodesign Directive.
- Project partners VTT and Aalto who have developed a new voltage divider for fast transients and a test system for puncture testing of cap-and-string insulators, which has been purchased by two commercial laboratories ABB (formerly STRI), Sweden and Verescence La Granja, Spain, both involved in insulator testing.
- Project partner PTB has provided feedback to AMOtronic a manufacturer of transient recorders for LI, especially regarding interference suppression.
- Project partner RISE has provided feedback to National Instruments, a manufacturer of fast transient recorders for general use, especially regarding step performance and stability of recorded level after the step. A step generator developed in the project has been central tool to this endeavour.
- Use of the new VSL CMC related to calibration of power TLM systems in on-site calibrations at the premises of Smit Transformatoren, a major manufacturer of power transformers and reactors.
- New CMCs have been announced for LI voltages, impulse currents, losses of reactors, power capacitors and power transformers and are expected to be approved by BIPM in early 2019.

Another (unexpected) project outcome resulted from the discussions in the CENELEC TC14 meetings. A need was expressed for further metrology research related to power transformers and reactor loss measurements. The need concerned better industrial systems, enhanced calibration accuracies of NMI reference setups to calibrate these systems, and further guidance in uncertainty evaluation of transformer loss measurements.

Concerning the uncertainty calculations, it was felt that the guidance provided by EN 60076-19 standard still is too complex for use by test engineers, and it furthermore lacks support in uncertainty evaluation of shunt reactor loss measurements. This discussion finally resulted in the formal expression of a standardisation research need to EMPIR:

[https://msu.euramet.org/current\\_calls/pre\\_norm\\_2017/documents/CEN\\_priorities/cen\\_priority\\_002.pdf](https://msu.euramet.org/current_calls/pre_norm_2017/documents/CEN_priorities/cen_priority_002.pdf)

Based on this need, a follow-up EMPIR project was formulated and approved for funding, 17NRM01 TrafoLoss.

#### **5.4 Impact on the metrological and scientific communities**

The outputs of the project include several important additions and extensions to CMC statements recorded in the BIPM key Comparison Database (KCDB). Specifically, new and extended CMCs are or will be submitted for:

- Measurement of losses at HV, high current and low power factor (150 kV, 2 kA, PF=0.01)
- Measurement of fast current transients (rise-time of 10 ns at currents of at least 50 A)
- Calibration of LI voltage measurement systems at UHV levels, i.e. above 2100 kV

These new CMCs provide a significant impact to the worldwide electrical power metrology community. As an example, the loss measurement setups developed in the project show that modern digital sampling systems have achieved sufficient accuracy to be successfully implemented in high-accuracy reference loss measurement systems. Their flexibility and enhanced automation are a significant advantage over the more traditional fully-analogue systems.

The project has hosted one workshop in cooperation with EMRP JRP ENG61 FutureGrid in August 2016 in Braunschweig, Germany. Altogether 40 people representing project partners, standardisation organisations, industry and academia attended the workshop, and 12 presentations and 23 posters were presented. A second workshop was held in Haarlem, the Netherlands in April 2018 and targeted graduate students, TSOs and stakeholders. The workshop was attended by 23 delegates, who benefited from 27 presentations and 14 posters.

#### **5.5 Impact on relevant standards**

The project has generated results that have provided valuable input to standardisation work within IEC and CENELEC. Liaisons have been accomplished by project partners, who are active in standardisation committees, such as CENELEC and IEC TC14 (power transformers), IEC TC20 (Electric cables), IEC TC42 (High-voltage and high-current test techniques), IEC TC22F WG25 (Determination of power losses in voltage source converters for HVDC systems), and CIGRÉ D1 WG60 (Traceable measurements of very fast transients).

The consortium is involved in an IEC Maintenance Team (MT) on “Rules for the determination of uncertainties in the measurement of losses in power transformers and reactors”, which has been charged with transferring an existing Technical Specification into a proper documentary standard. The project coordinator is the convenor of this Maintenance Team with project partner VSL a member.

Findings both for LI and for fast transients have been presented to plenary meetings of IEC TC42. Further contributions will be presented to IEC TC42 for consideration of amendments to international standardisation, especially in the upcoming revision of IEC 60060-2, where several project partners expect to take part.

#### **5.6 Potential impact**

##### **5.6.1 Instrumentation**

In the field of LI measurements, the project has developed the metrological infrastructure for manufacturers of LI test equipment to reliably verify their equipment for UHV that are required by the manufacturers of UHV grid components. This is an enabler for TSO to set up grids with lower losses and to have reliable grid components for such grids.

The reference setups for transformer, reactor, capacitor, and cable loss measurements of are a major step forward in the development of a full metrological infrastructure for loss measurements of grid components. It is expected that more requirements will be set by EU legislation and by utility companies on the losses of grid components. Therefore this project provides the manufacturers of such grid components with the required tools to unambiguously prove that their products indeed meet present efficiency requirements.

### 5.6.2 Environmental

By developing reference setups for the verification of HV and UHV equipment, the project has provided a basis for achieving one of the “20/20/20” targets of the EU, a 20 % reduction in CO<sub>2</sub> emissions by the year 2020. Transmission grid power transformers are responsible for a sizeable part of grid losses, and this project provides support for the design, development, and realisation of improved, lower-loss transformers. Even the smallest contribution to this improvement can result in a reduction in CO<sub>2</sub> emissions of many kilotons per year.

The achievement of further environmental impact has been stimulated by supporting the development of (U)HV transmission grids via the new (U)HV LI reference facilities. (U)HV grids are crucial for the large-scale introduction of renewable energy sources, such as in wind parks, solar panel parks. In turn supporting having more electricity supplied by renewable energy sources meaning that less conventional carbon-rich electricity generation, by for example coal plants, is required and less CO<sub>2</sub> is emitted.

### 5.6.3 Financial

The project has supported the competitiveness of the European HV grid transmission industry through the development of loss measurement facilities and extending HV testing facilities, based on stakeholder needs and requirements in recent written standards. For example, the direct calibration of their power transformer loss facilities was a crucial selling point for Royal Smit Transformatoren B.V. in the Netherlands, which led them to actively support the VSL development of a reference setup for calibration of their industrial TLM systems. Such a calibrations to internationally recognised measurement standards have supported the proven determination of the losses in the HV power transformers being purchasing. This requirement was recognised by CENELEC TC14, who decided to develop – with support from the project – the EN 60076-19 for uncertainty evaluation of TLM systems in order to fully support the requirements of the Ecodesign Directive.

Similarly, the improved HV testing facilities support European manufacturers in their status at the forefront of HV transmission grid innovation. HV transmission grids are rapidly moving to higher and higher voltages, urging the need for a supporting metrology infrastructure, such as developed in this project.

A further significant financial project impact relates to grid losses. The losses in the European electricity grids of 300 TWh/year correspond to a financial loss of 15000 M€/year (typical electricity cost is 50 €/MWh). Even if the metrological infrastructure developed in the project only contributes to a 0.01 % reduction of the grid losses e.g. through the better design of HVDC convertors and HV power transformers, the annual financial gain would exceed the cost of this project.

### 5.6.4 Social

Reliable electrical delivery is one of the prime needs in modern society; it is at least as important as water supplies, as the latter depends on the supply of electricity. HV transmission grids are the backbone of the total electricity grid infrastructure and are often referred to as the most extensive and complex machine made by humankind.

However, the current grid infrastructure is aging, and the addition of renewable energy sources stresses the grid, affecting the reliability of our daily electricity supply. Therefore, there is an urgent need for further development of the transmission grid infrastructure. This project has supported this development by providing the required measurement tools and calibration facilities needed for reliable design and production of future electrical grids, which in turn contributes to the prevention of blackouts.

### 5.6.5 Political

The project's results have provided a solid basis for the realisation of all three 20/20/20 aims made by EU politicians: 20 % less CO<sub>2</sub> emission, 20 % energy saving (lower losses), and 20 % energy production from renewable energy sources by the year 2020. As already stated above, the new facilities for reliable determination of losses in transmission grid components support the development of new grid components with improved loss behaviour. This contributes to lower losses (energy saving) as well as to reduced CO<sub>2</sub> emission, since less electricity needs to be produced to provide for the losses in the transmission grid. The project also supports the development of UHV transmission grids with even higher voltages, where losses are lower with respect to present HV grids.

Moreover, HV transmission grids are vital for the large-scale introduction of renewable energy sources in total energy production. The increased use of renewable energy allows Europe to be more self-supporting and less dependent on carbon-rich conventional energy sources, such as oil. For example, local electricity generation by e.g. solar panels on the roofs of houses, already provides a sizeable contribution to such renewable generation, and a major contribution is made by large wind parks. In the course of the project large-scale wind

generation has sharply increased, with single wind parks exceeding the production of a conventional (coal) power plant. Since such wind parks are generally located far away from the major electricity consumers therefore, HV transmission grids are crucial for providing the “highway” for transportation of the electricity generated by large-scale renewables, and thus realising the EU’s 20/20/20 energy aims.

## 6 List of publications

- [1]. E. Houtzager, M. Acanski, and G. Rietveld, "Reference setup for the calibration of power transformer loss measurement systems" CPEM 2016-07-10—15, Ottawa, Canada, DOI '10.1109/CPEM.2016.7540487
- [2]. Gert Rietveld, Ernest Houtzager, and Dongsheng Zhao, "Impact of the Ecodesign Directive on Traceability in Power Transformer Loss Measurements", in *CIREC 2015 conference, 1-18 June 2015, Lyon, France*.
- [3]. E. Mohns, J. Hällström, E.-P. Suomalainen, H. Badura, and S. Fricke, "Precision Loss Measurement of Reactive Compensation Components by Sampling Voltage and Current", CPEM 2016-07-10—15, Ottawa, Canada, DOI '10.1109/CPEM.2016.7540545
- [4]. G. Rietveld, E. Houtzager, M. Acanski, and D. Hoogenboom, "Meeting Ecodesign Efficiency Requirements: Ensuring Accuracy in Power Transformer Loss Tests via TLM System Calibrations" CIREC 2017, Glasgow, Scotland, 12-15 June 2017.
- [5]. E. Mohns, P. Räther, H. Badura, M. Schmidt, "Standard for High-Power Loss Measurement Systems for Testing Power Transformers" IEEE AMPS 2016 workshop, Aachen, Germany, DOI '10.1109/AMPS.2016.7602858
- [6]. J. Havunen, J. Hällström, A. Bergman, A. E. Bergman, "Using Deconvolution for Correction of Non-Ideal Step Response of Lightning Impulse Digitizers and Measurement Systems", ISH 2017 Buenos Aires, Argentina, 2017-08-28—09-01
- [7]. J. Hällström, S. Kazmi, M-L Pykälä, J. Havunen, "Design and performance of a fast divider for puncture testing", ISH 2017 Buenos Aires, Argentina, 2017-08-28—09-01
- [8]. A. Bergman, M. Nordlund, A-P. Elg, J. Meisner, S. Passon, J. Hällström "Characterization of a fast step generator", ISH 2017 Buenos Aires, Argentina, 2017-08-28—09-01
- [9]. M. Nordlund, A. Bergman, A-P. Elg, J. Havunen, J. Hällström, J. Meisner, "Influence of coaxial cable on response of high voltage resistive dividers", ISH 2017 Buenos Aires, Argentina, 2017-08-28—09-01
- [10]. A. Bergman, A-P. Elg, J. Hällström, J. Meisner, "Evaluation of step response of transient recorders for lightning impulse", ISH 2017 Buenos Aires, Argentina, 2017-08-28—09-01
- [11]. W. Larzelere, J. Hällström, A-P. Elg, A. Bergman, J. Klüss, Y. Li, L. Zhou, H. Gao, "Measurement of the Internal Inductance of Impulse Voltage Generators and the Limits of LI Front Times" ISH 2017 Buenos Aires, Argentina, 2017-08-28—09-01
- [12]. J. Meisner, C. Schierding, "PTB's new standard impulse voltage divider for traceable calibrations up to 1 MV", ISH 2017 Buenos Aires, Argentina, 2017-08-28—09-01
- [13]. Gert Rietveld and Ernest Houtzager, "High-accuracy reference setup for system calibration of transformer loss measurement systems", ISH 2017 Buenos Aires, Argentina, 2017-08-28—09-01
- [14]. E. Mohns, P. Räther, H. Badura, "An AC Power Standard for Loss Measurement Systems for Testing Power Transformers", IEEE Transactions on Instrumentation and Measurement ( Volume: PP, Issue: 99 ), DOI: 10.1109/TIM.2017.2698678
- [15]. A. Bergman, M. Nordlund, "Characterisation at low voltage of two reference lightning impulse dividers", ISH 2017 Buenos Aires, Argentina, 2017-08-28—09-01, [https://e-cigre.org/publication/ISH2017\\_485-characterisation-at-low-voltage-of-two-reference-lightning-impulse-dividers](https://e-cigre.org/publication/ISH2017_485-characterisation-at-low-voltage-of-two-reference-lightning-impulse-dividers)

## 7 Website address and contact details

<http://GridMeas.eu/>

RISE Research Institutes of Sweden, Dr. Anders Bergman, P.O. Box 857, SE-501 15 BORÅS, Sweden

Email: [anders.bergman@ri.se](mailto:anders.bergman@ri.se)